

Fission Cross Sections

Paul Lisowski

Guest Scientist, Los Alamos National
Laboratory

Outline

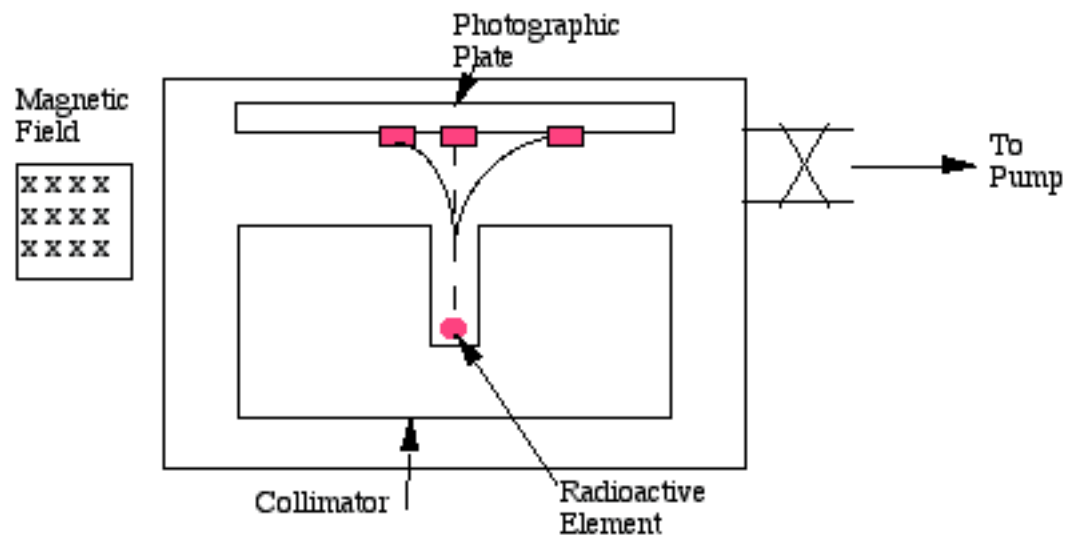
- Introduction – events leading to experimental evidence of nuclear fission
- Fission Phenomenology and Observables
- Fission Cross Sections Using Neutrons
- Fission Cross Sections from Charged Particle Measurements
- The Future of Fission Cross Section Measurements and Possible Improvements

Introduction – Some Key Events

1896: Becquerel accidentally discovers radioactivity from uranium ore and discovers that deflection in a magnetic field led to positive, negative, and neutral classes of radioactivity.

1905: Einstein publishes mass-energy equivalence paper.

1906: Rutherford develops his model of the atom, which led him to conclude that positive charge is concentrated in a small nucleus.
1920: Rutherford has a book on the disintegration of atoms and the number of atoms in a sample.



Introduction – Some Key Events

1896: Becquerel accidentally discovers radioactivity from uranium ore and discovers that deflection in a magnetic field led to positive, negative, and neutral classes of radioactivity.

1905: Einstein publishes mass-energy equivalence paper.

1906: Rutherford discovers α particles and develops scattering apparatus – results lead him to conclude that atoms have a nucleus of positive charge.

Einstein, A. (1905), "Ist die Trägheit eines Körpers von seinem Energieinhalt abhängig?", *Annalen der Physik*, **18**: 639–643

1920: Rutherford postulates that the nucleus has a bound 'electron-proton pairs' to explain the disparity between element's atomic mass and number.

Or:

Does the inertia of a body depend upon its energy-content?



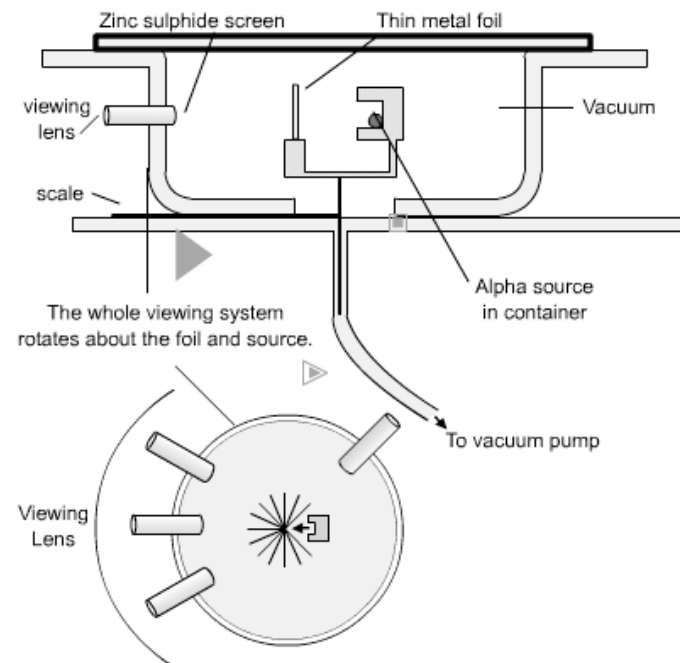
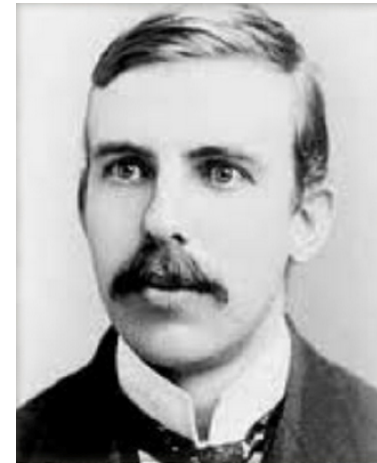
Introduction – Some Key Events

1896: Becquerel accidentally discovers radioactivity from uranium ore and discovers that deflection in a magnetic field led to positive, negative, and neutral classes of radioactivity.

1905: Einstein publishes mass-energy equivalence paper.

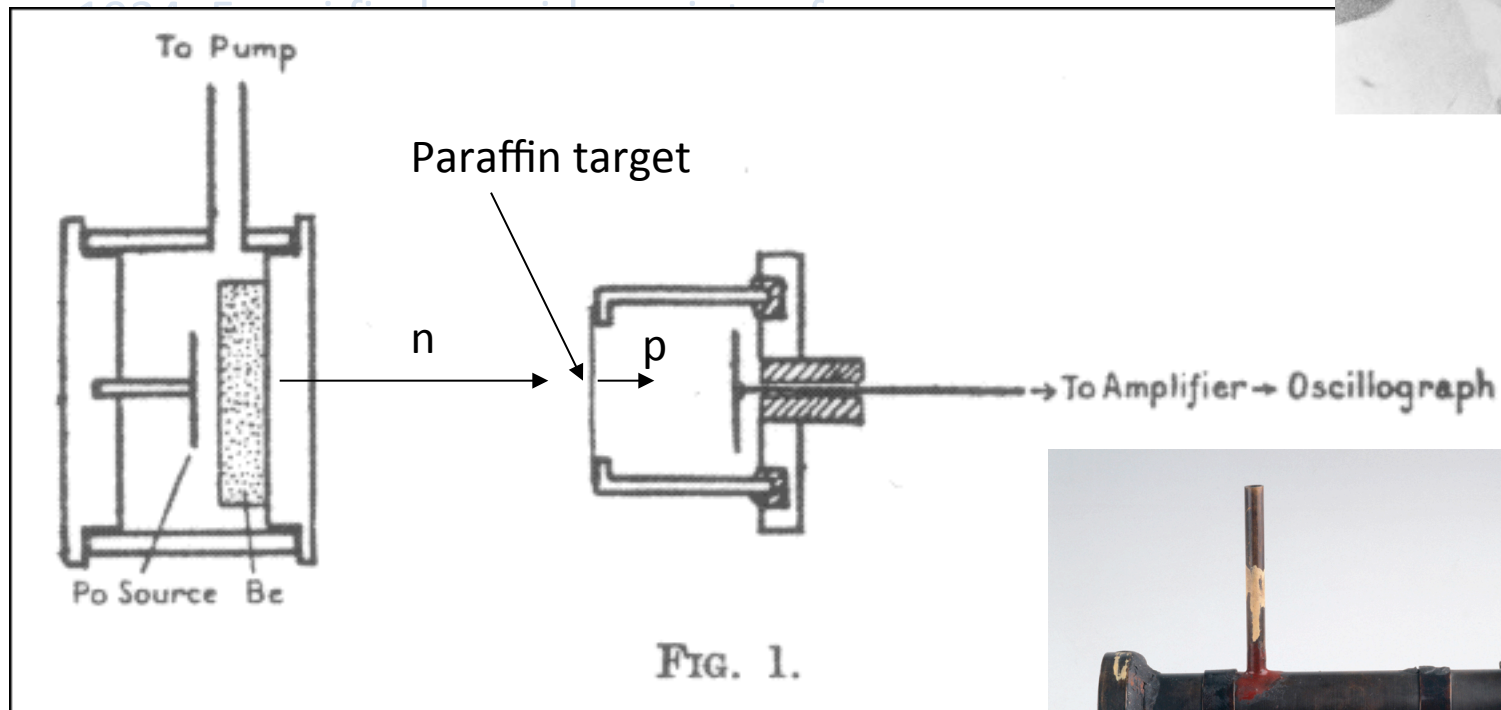
1906: Rutherford discovers α particles and develops scattering apparatus – results lead him to conclude that atoms have a ‘nucleus’ of positive charge.

1920: Rutherford postulates that the nucleus has bound ‘electron-proton pairs’ to explain the disparity between element’s atomic mass and number.



Introduction – Some Key Events

1932: Chadwick bombards Beryllium with α particles: proposes that the 'electron-proton pairs' were really a new particle – the neutron.



1939: Lise Meitner and Otto Frisch explain the process as neutron capture leading to uranium splitting, calculating a 200 MeV energy release



Introduction – Some Key Events

1932: Chadwick bombards Beryllium with α particles: proposes that the ‘electron-proton pairs’ were really a new particle – the neutron.

1934: Fermi finds a wide variety of radionuclides from irradiating uranium using a Po-Be source including lighter elements

1934: Ida Noddack publishes a paper discussing Fermi’s radiochemistry and suggests ‘It is conceivable that the nucleus breaks up into several large fragments ...’

1938: Otto Hahn and Fritz Strassmann irradiate uranium and show that the lighter elements seen by Fermi were about $\frac{1}{2}$ the mass of the uranium, demonstrating fission

1939: Lise Meitner and Otto Frisch explain the process as neutron capture leading to uranium splitting, calculating a 200 MeV energy release.



Introduction – Some Key Events

1932:

particle
pairs

1934:

radio

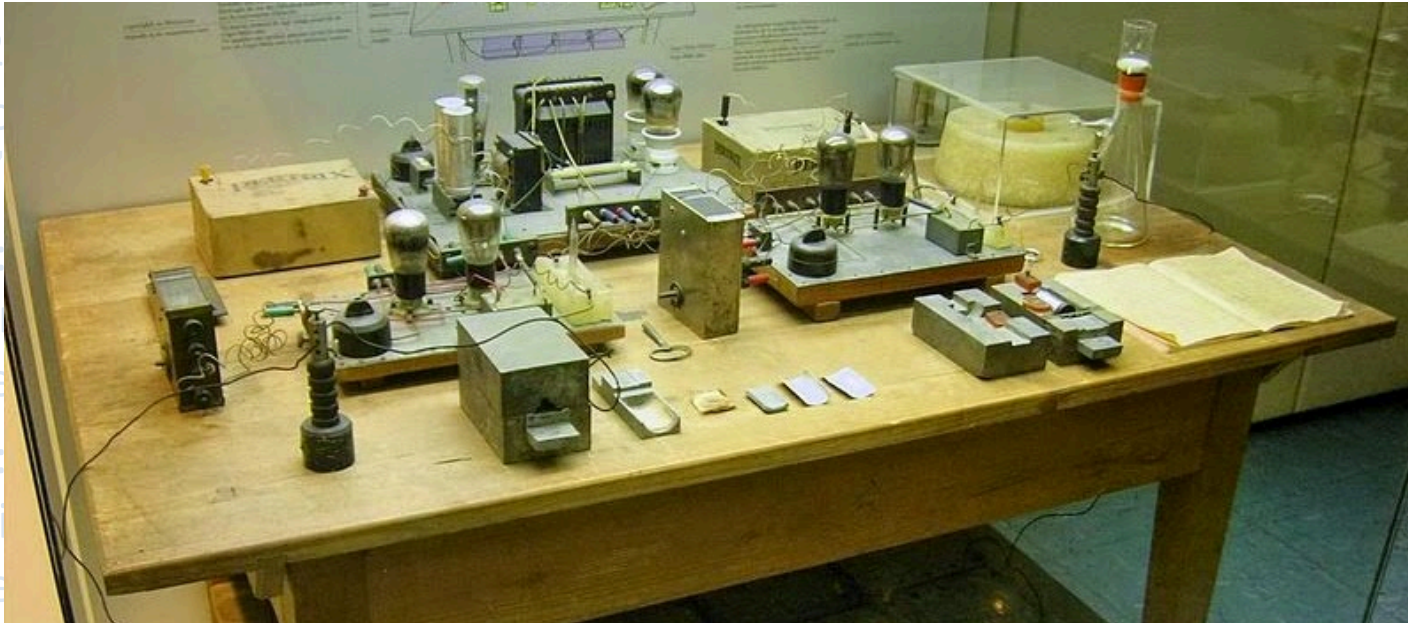
Po-Bi

1934:

Fermi

conce

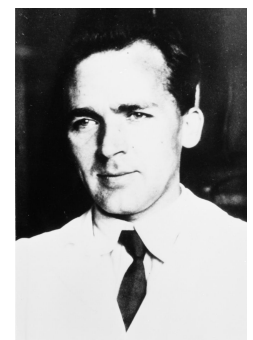
several large fragments ...”



1938: Otto Hahn and Fritz Strassmann irradiate uranium with neutrons and identify Barium, showing that the lighter elements earlier seen by Fermi were about 1/2 the mass of the uranium, demonstrating fission.



Hahn



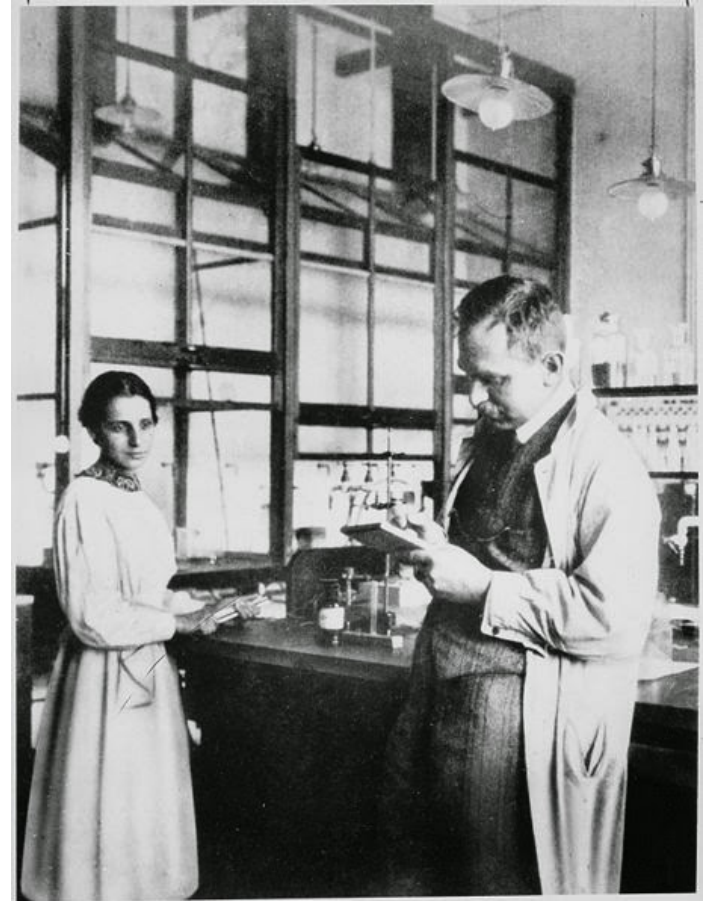
Strassmann

Introduction – Some Key Events

1938: Lise Meitner and Otto Frisch explain the process as neutron capture leading to uranium splitting, calculating a 200 MeV energy release.

1939: Frish provides experimental confirmation of of the energy release, confirming Einstein's 1905 paper.

1939: Ladenberg, Kanner, Barschall, and Van Voorhies publish the first measurements of the reaction probability of 2-3 MeV neutrons of Uranium.



Introduction – Some Key Events

1939: Lise Meitner and Otto Frisch explain the process as neutron capture leading to uranium splitting, calculating a 200 MeV energy release.

1939: Frish provides experimental confirmation of of the energy release, confirming Einstein's 1905 paper.

1939: Bohr and Wheeler publish the first theoretical analysis of the mechanism of nuclear fission based on the liquid drop model

1939: Ladenberg, Kanner, Barschall, and Van Voorhies publish the first measurements of the reaction probability of 2-3 MeV neutrons of Uranium.



Introduction – Some Key Events

1939: Lise Meitner and Otto Frisch explain the process as neutron capture leading to uranium splitting, calculating a 200 MeV energy release.

1939: Frish provides experimental confirmation of the energy release, confirming Einstein's 1905 paper.

1939: Bohr and Wheeler publish the first theoretical analysis of the mechanism of nuclear fission based on the liquid drop model

1939: Ladenberg, Kanner, Barschall, and Van Voorhies publish the first measurements of the reaction probability for 2-3 MeV neutrons of Uranium.

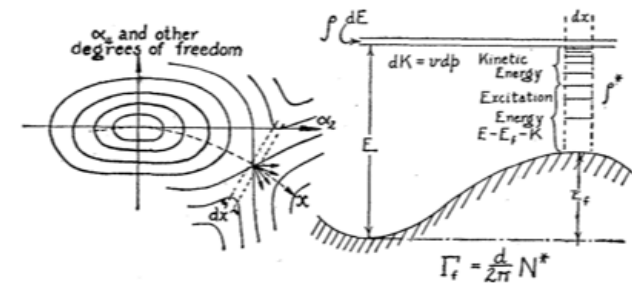


FIG. 3. The potential energy associated with any arbitrary deformation of the nuclear form may be plotted as a function of the parameters which specify the deformation, thus giving a contour surface which is represented schematically in the left-hand portion of the figure. The pass or saddle point corresponds to the critical deformation of unstable equilibrium. To the extent to which we may use classical terms, the course of the fission process may be symbolized by a ball lying in the hollow at the origin of coordinates (spherical form) which receives an impulse (neutron capture) which sets it to executing a complicated Lissajous figure of oscillation about equilibrium. If its energy is sufficient, it will in the course of time happen to move in the proper direction to pass over the saddle point (after which fission will occur), unless it loses its energy (radiation or neutron re-emission). At the right is a cross section taken through the fission barrier, illustrating the calculation in the text of the probability per unit time of fission occurring.

Fission Phenomenology and Observables

Liquid Drop Model

The liquid drop model developed by Gamow and formulated by Weizsäcker in 1935 treats the nucleus as a uniformly charged incompressible liquid drop with the total binding energy of the nucleus given as:

$$B = a_v A - a_s A^{2/3} + a_c \frac{Z(Z-1)}{A^{1/3}} - a_a \frac{(A-2Z)^2}{A} \pm \delta(A, Z)$$

Volume

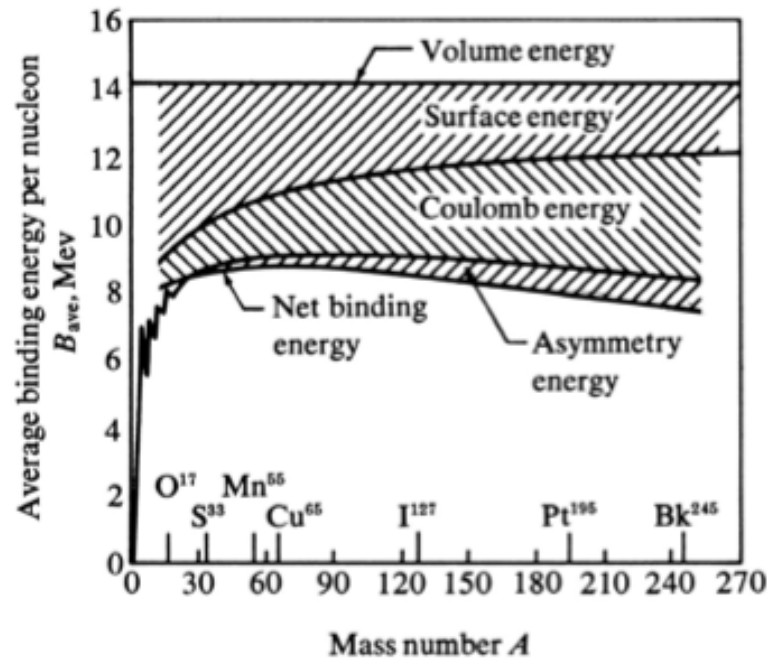
Surface

Coulomb

Isospin

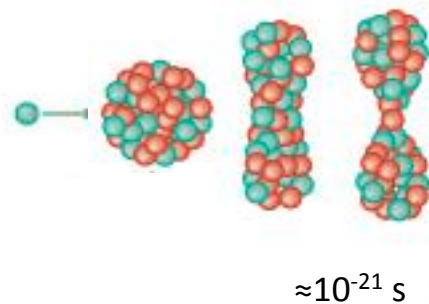
Pairing

In 1939, Bohr and Wheeler applied this model to explain fission which occurs when the nucleus stretches and oscillates. For a liquid drop, of constant volume, deformation information matters, so only the Coulomb and surface energy terms are important as the nucleus is stretched.

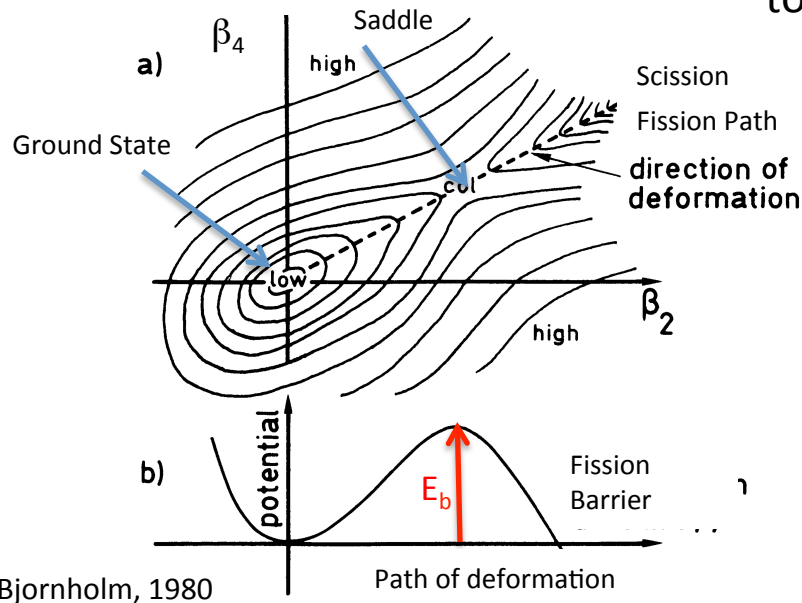


Fission Phenomenology and Observables

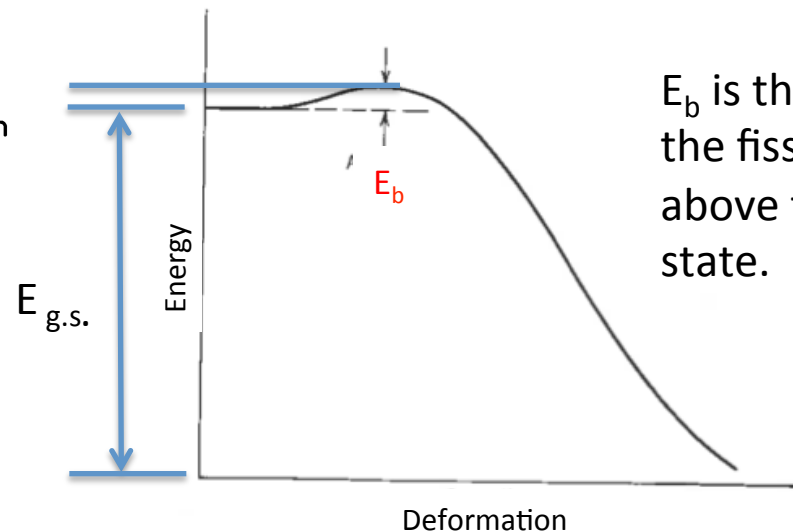
Bohr and Wheeler Model of a Neutron-Induced Fission Event



With the deformation energy in the liquid drop as the difference between the surface and Coulomb terms, Bohr and Wheeler described the nuclear deformation by a Legendre expansion about the nuclear radius $R(\theta)$ with coefficients β_n . In the $(\beta_2 - \beta_4)$ plane they found a saddle point. Beyond that the minimum energy path slopes downward allowing the nucleus to break apart. The fissioning nucleus just has to have enough energy to overcome the fission barrier E_h .



Bjornholm, 1980

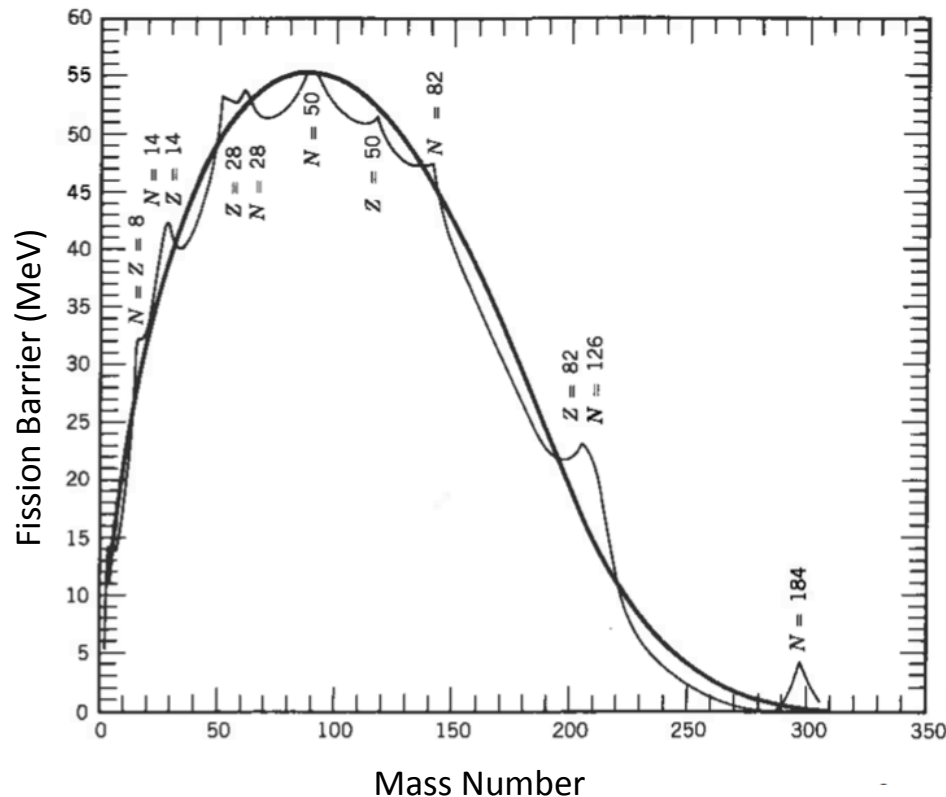


E_b is the height of the fission barrier above the ground state.

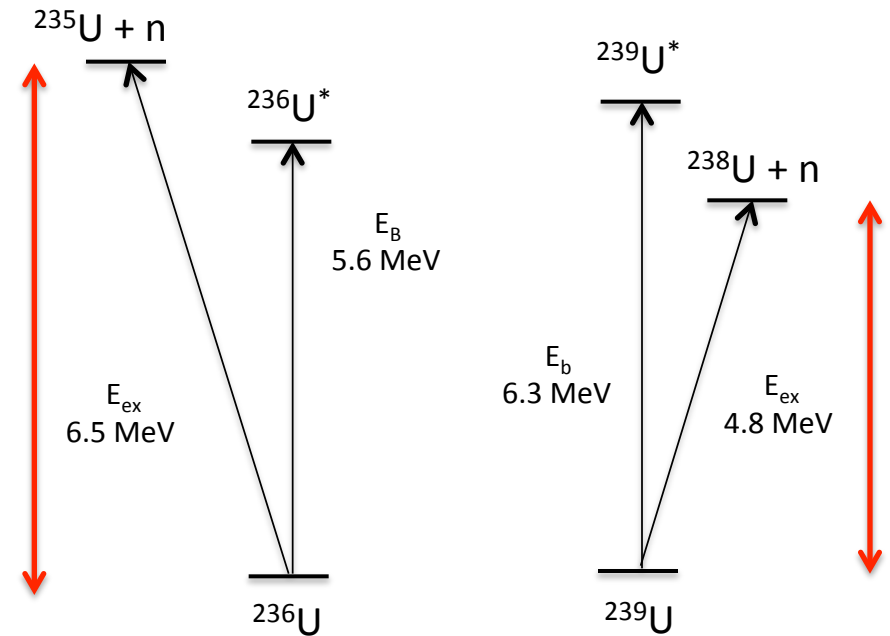
Fission Phenomenology and Observables

Fission Barrier Heights and Energy Level Diagrams for ^{235}U and ^{238}U

Formation of $^{236}\text{U}^*$ and $^{239}\text{U}^*$ can lead to fission.



Fission Barrier Height variation with mass number calculated from LDM for the most stable isotope at each mass number. The light curve includes shell structure. Myers Nucl Phys, 81, 1 (1966)

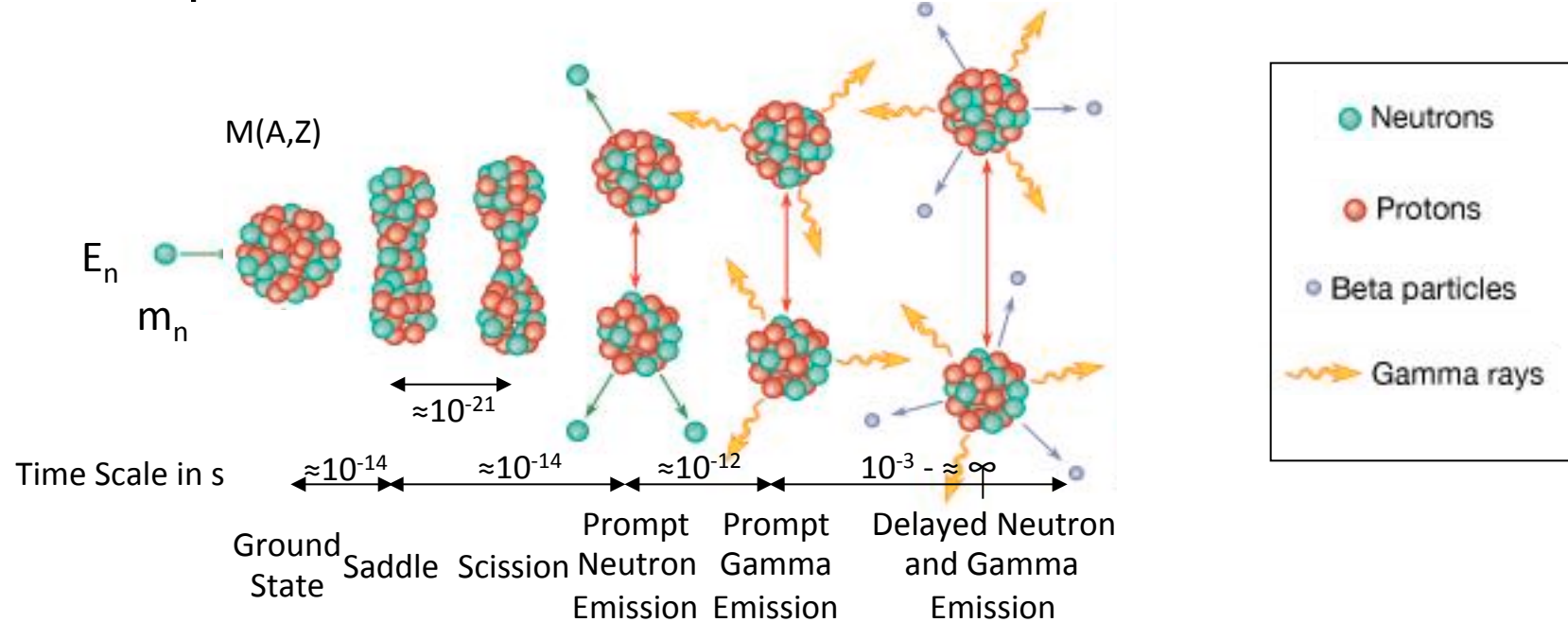


$^{235}\text{U} + n$ has a higher energy than the lowest fissionable state, so it can fission with a zero-energy neutron

$^{238}\text{U} + n$ has a lower energy than the lowest fissionable state, so it requires additional 1.5 MeV of kinetic energy to fission

Fission Phenomenology and Observables

A Simple Picture of a Neutron-Induced Fission Event



Total available energy: $E_t = [M(Z,A) - M_L(Z_L,A_L) - M_H(Z_H,A_H) + m_n] c^2 + E_n$

The fission fragments are generally left in an excited state and the energy is distributed between the kinetic energy and excitation energy, denoted as E_{TKE} and E_{TXE} .

Where E_{TXE} is the total fragment internal energy resulting from the fragments changing to their equilibrium deformation after scission.

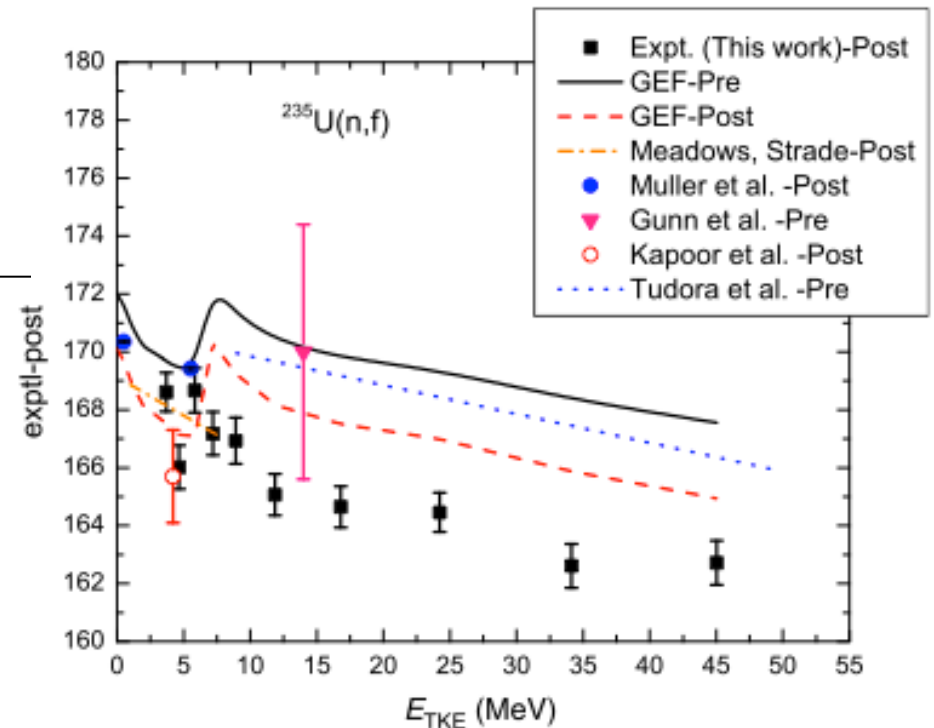
Fission Phenomenology and Observables

Fission Energy Release

^{235}U thermal neutron fission

Approximate Prompt Energy Release	MeV
Fission Fragments	170
Fission Neutrons	5
Prompt γ emission	7
γ emission from fission fragments	7
β emission from fission fragments	8
ν from fission products	12
Total Energy per Fission	209

When resulting from more energetic particles the energy released by fission fragments has an energy dependence, shown here for post neutron emission.



Excitation energy dependence of the total kinetic energy release in $^{235}\text{U}(n,f)$ Yanez, 2014

See also Madland, 2006

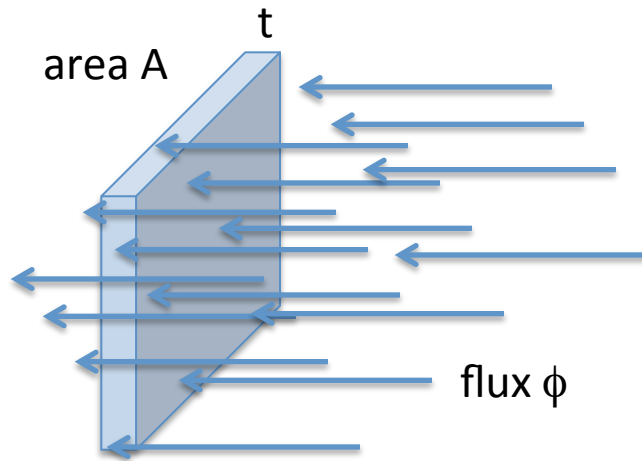
Fission Phenomenology and Observables

Fission has a complex set of observables, measurements of each of which provide information that helps us understand the overall process

- Energy Release
- Fission cross sections and probabilities for different incident particles and energies
- Multiplicity, Energy, and Angle Distributions of Neutrons and Gamma Rays from Fission
- Fragment Kinetic Energy, Mass, and Charge Yields and Angular Distributions
- Fragment Delayed Neutrons
- Fragment Beta and Gamma Decay Processes
- Spontaneous Fission
- Spin and parity distributions of fission resonances
- Parity violation in fission resonances
- Fission Time Scales
- ...

Fission Phenomenology and Observable

Cross Sections



$$I = \phi \cdot A \text{ (number of particles/s)}$$

The interaction rate R for incident particles on a surface of area A and thickness t depends on the intensity and the number of nuclei exposed to the incident particles:

The intensity I (number of particles/s) is defined in terms of a flux ϕ , or number of particles/cm²/s striking an area A

For N_t target nuclei with number density ρ (#/cm³) exposed to the incident particles, then

$$N_t = \rho \cdot A \cdot t$$

The interaction rate R will be proportional to the number of incident particles (I) and number of atoms (n)

$$R \propto \phi \cdot N_t$$

$$R \propto \phi \cdot \rho \cdot A \cdot t$$

$$R = \sigma \cdot \rho \cdot A \cdot t \cdot \phi$$

σ = event rate per atom/incident flux with units of area

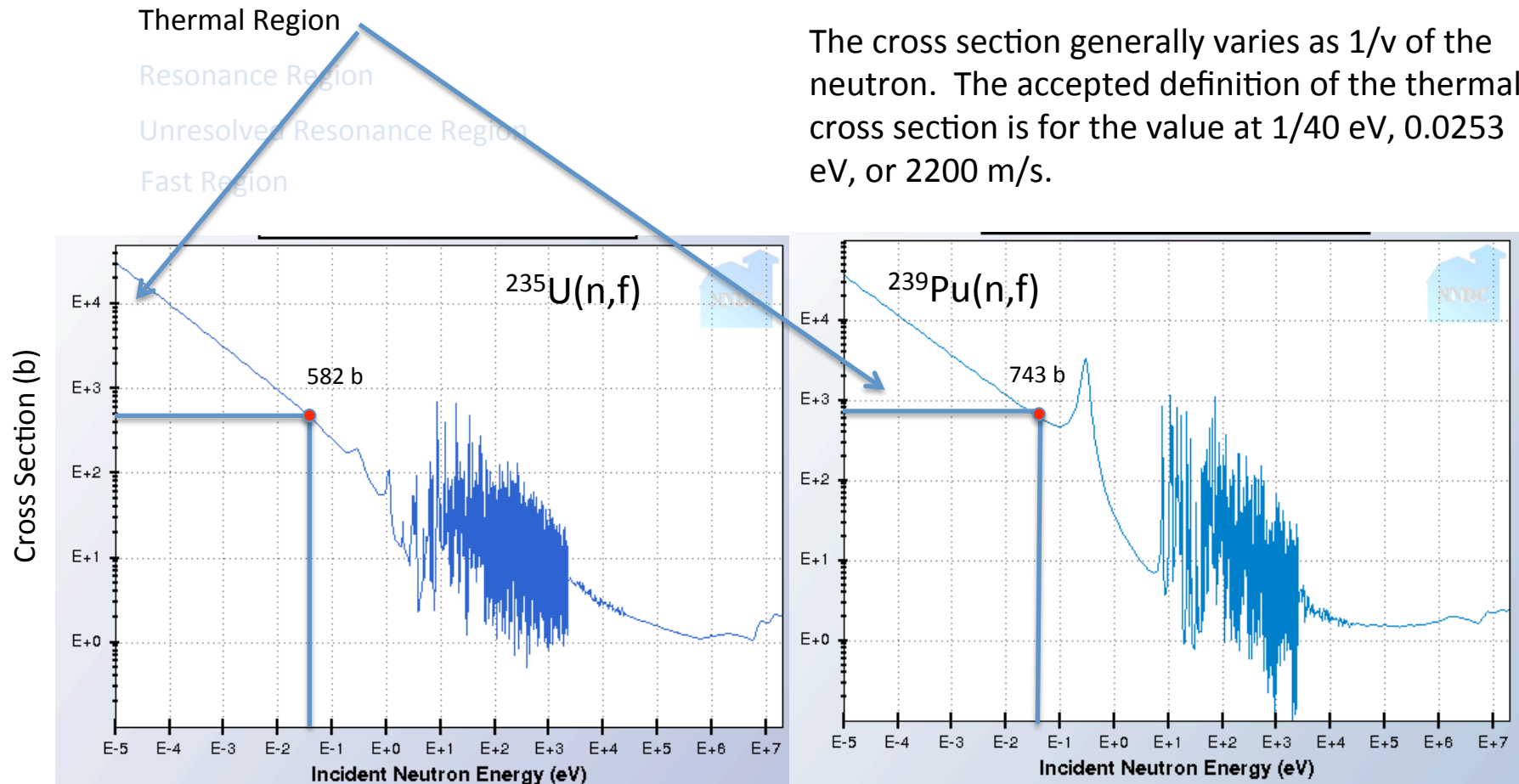
It is the probability that a particle will interact with a nucleus, or the effective cross sectional area of the nucleus. Units are barns or 10⁻²⁴ cm²

Note: $R = \sigma \cdot N_t \cdot \phi$

Fission Phenomenology and Observables

Neutron Induced Fission Cross Sections have a complex energy dependence

The cross section generally varies as $1/v$ of the neutron. The accepted definition of the thermal cross section is for the value at 1/40 eV, 0.0253 eV, or 2200 m/s.



<http://www.nndc.bnl.gov/sigma/>
ENDF/B-VII.1

Fission Phenomenology and Observables

Neutron Induced Fission Cross Sections have a complex energy dependence

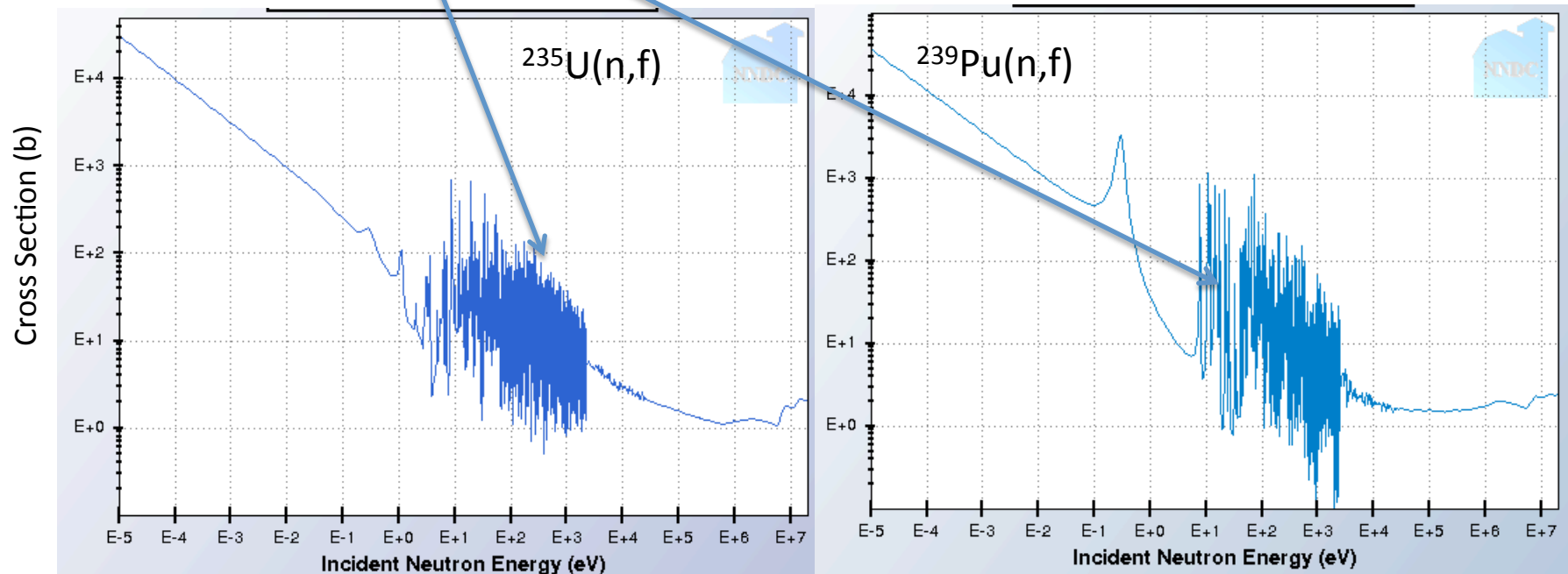
Thermal Region

Resonance Region

Unresolved Resonance Region

Fast Region

Characterized by narrow structure associated with energy levels in the compound nucleus. Experiments can resolve individual resonances and the data is generally represented by resonance parameters based on R-matrix theory.



<http://www.nndc.bnl.gov/sigma/>
ENDF/B-VII.1

Fission Phenomenology and Observables

Neutron Induced Fission Cross Sections have a complex energy dependence

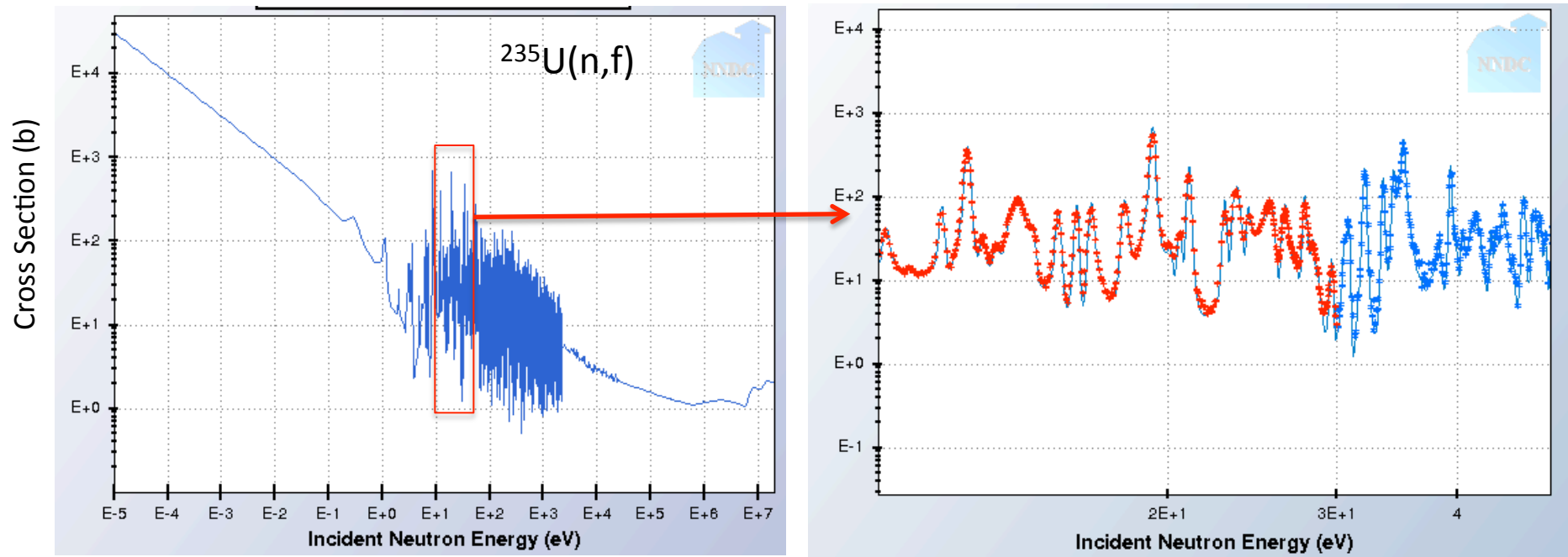
Thermal Region

Resonance Region

Unresolved Resonance Region

Fast Region

Expansion of resonance region for ^{235}U showing ENDF/B-VII.1 evaluation (solid line) and one set of experimental data from Wagemans (1979)



<http://www.nndc.bnl.gov/sigma/>
ENDF/B-VII.1

Fission Phenomenology and Observables

Neutron Induced Fission Cross Sections have a complex energy dependence

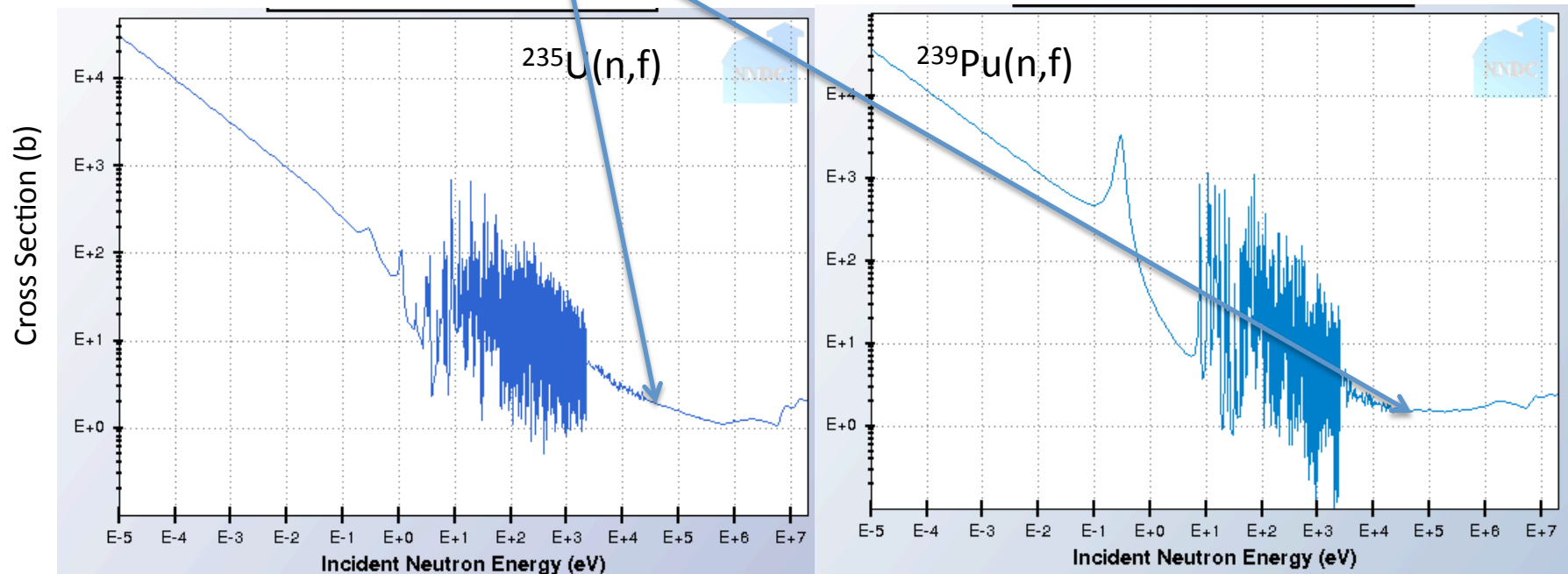
Thermal Region

Resonance Region

Unresolved Resonance Region

Fast Region

In this region the cross section still fluctuates, but levels in the compound nucleus are too closely spaced to be resolved. The cross section is approximated by average resonance parameters using statistical and level density models.



<http://www.nndc.bnl.gov/sigma/>
ENDF/B-VII.1

Fission Phenomenology and Observables

Neutron Induced Fission Cross Sections have a complex energy dependence

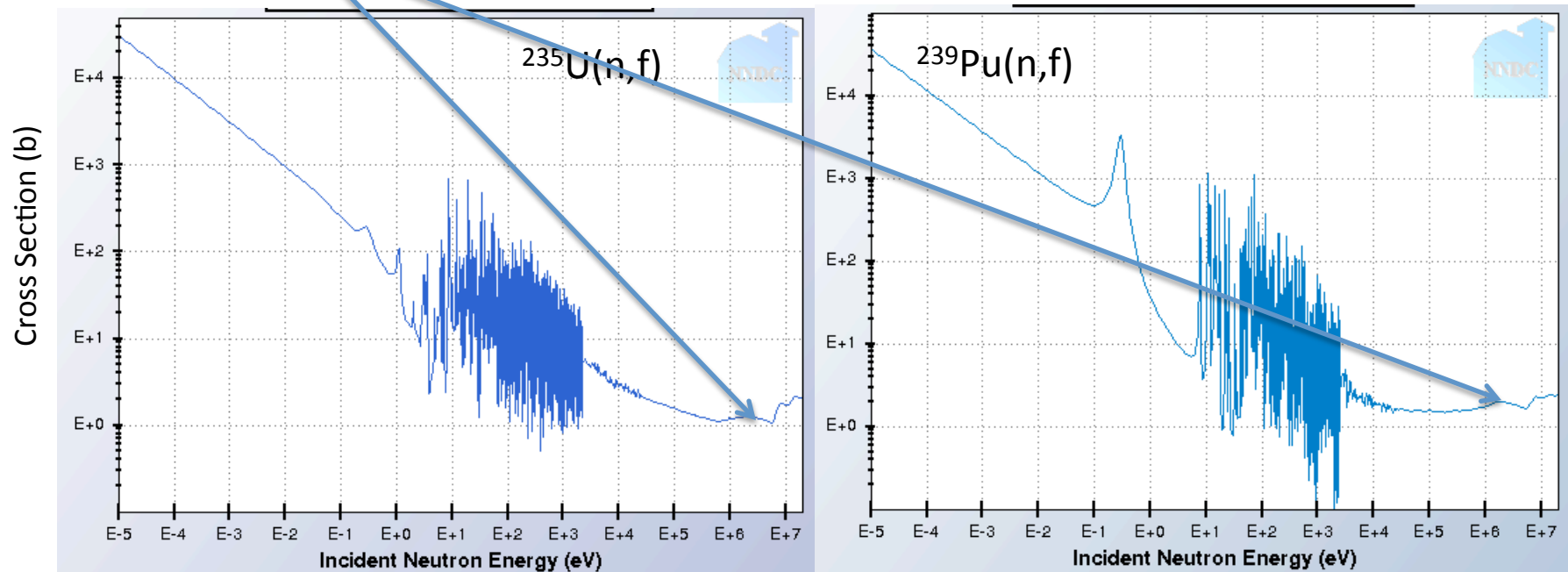
Thermal Region

Resonance Region

Unresolved Resonance Region

Fast Region

Levels overlap so strongly that there are no longer fluctuations, cross sections are smooth. They are represented by statistical, intra-nuclear cascade, pre-equilibrium, and evaporation models.



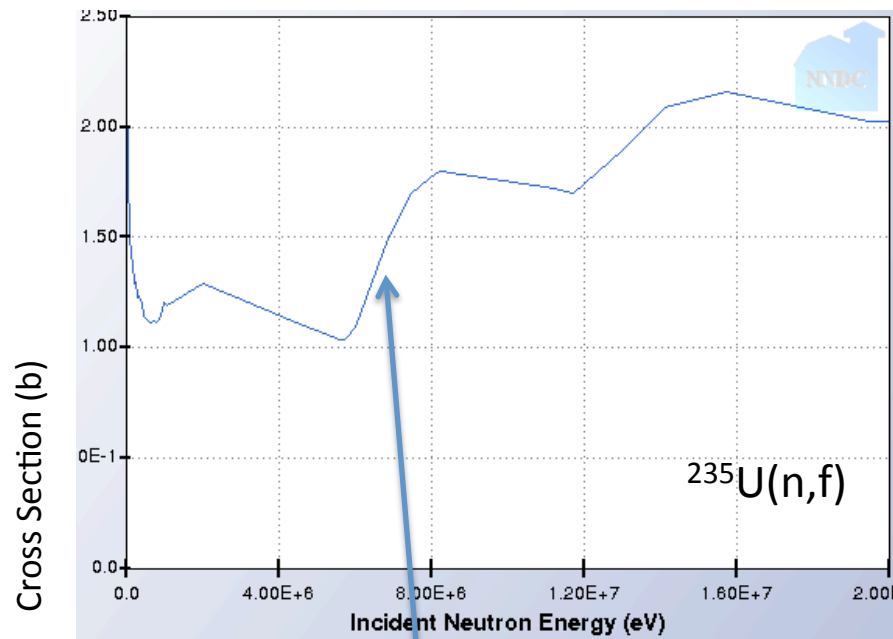
<http://www.nndc.bnl.gov/sigma/>
ENDF/B-VII.1

Fission Phenomenology and Observables

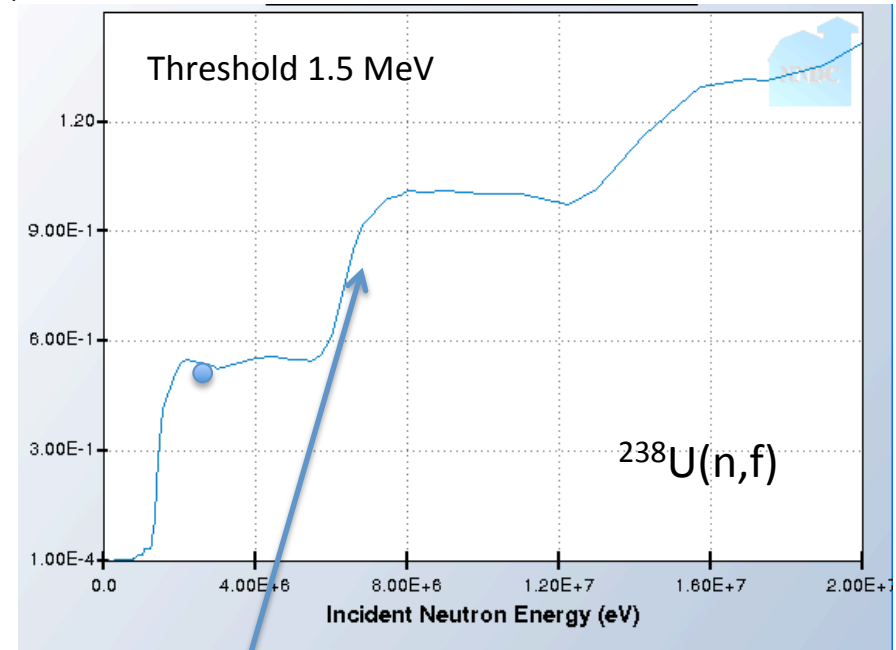
Multiple Chance Fission

<http://www.nndc.bnl.gov/sigma/>

ENDF/B-VII.1



Second chance fission



Second chance fission

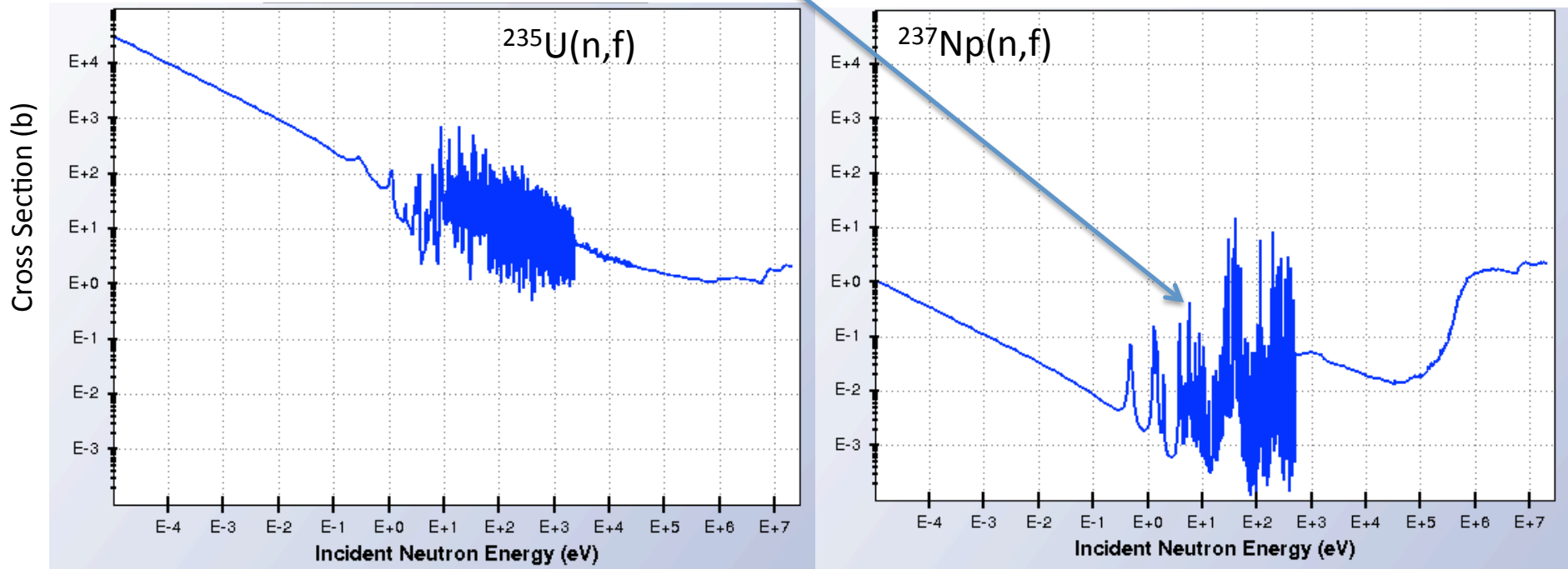
Fast neutron induced fission is generally smooth with regular steps as the incident neutron energy increases enough to allow the compound nucleus to emit one neutron and still have enough energy to fission (n,n'f). This is 'second chance' fission. At higher incident energies, 'third chance' fission becomes possible.

Fission Phenomenology and Observables

Subthreshold fission Resonances

The simple fission barrier model of Bohr and Wheeler does not allow fission for neutron energies below a 'threshold' for nuclei like ^{237}Np .

In reality, subthreshold fission resonances are observed, but with substantially lower cross section values than for fissile nuclei.



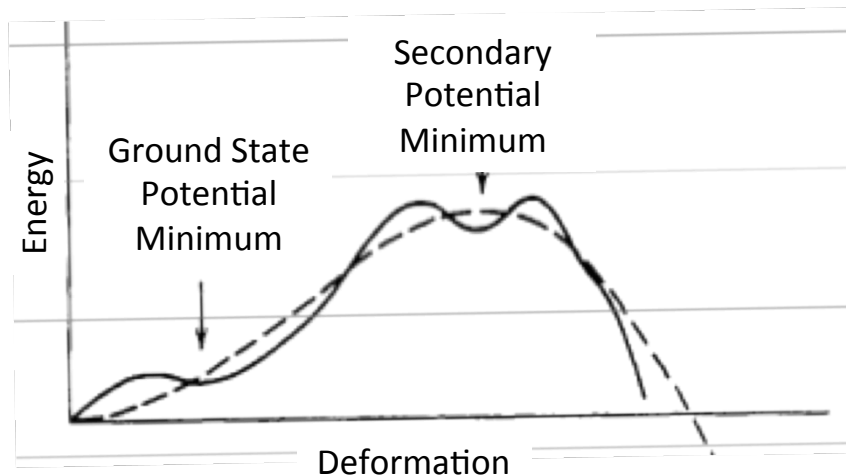
<http://www.nndc.bnl.gov/sigma/>

ENDF/B-VII.1

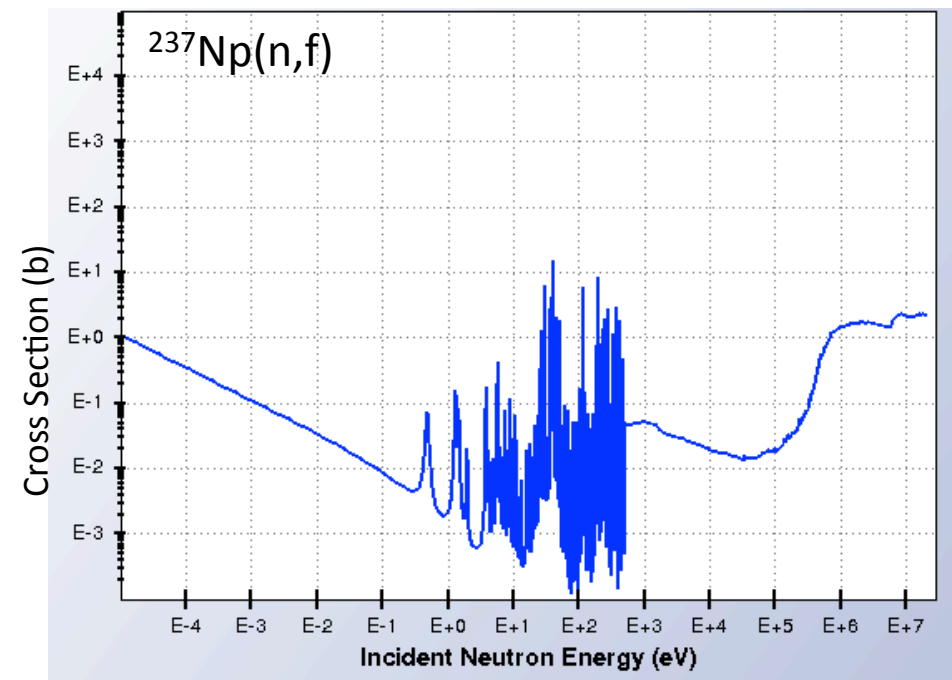
Fission Phenomenology and Observables

Subthreshold fission Resonances

In 1967 Strutinsky pointed out that the true fission barrier is more complicated than the simple LDM shape and added shell model corrections giving a double-humped barrier.



Having a double-humped fission barrier changes the fission barrier penetrability calculation giving transmission resonances at energies corresponding to vibrational states in the second well and giving rise to subthreshold fission resonances

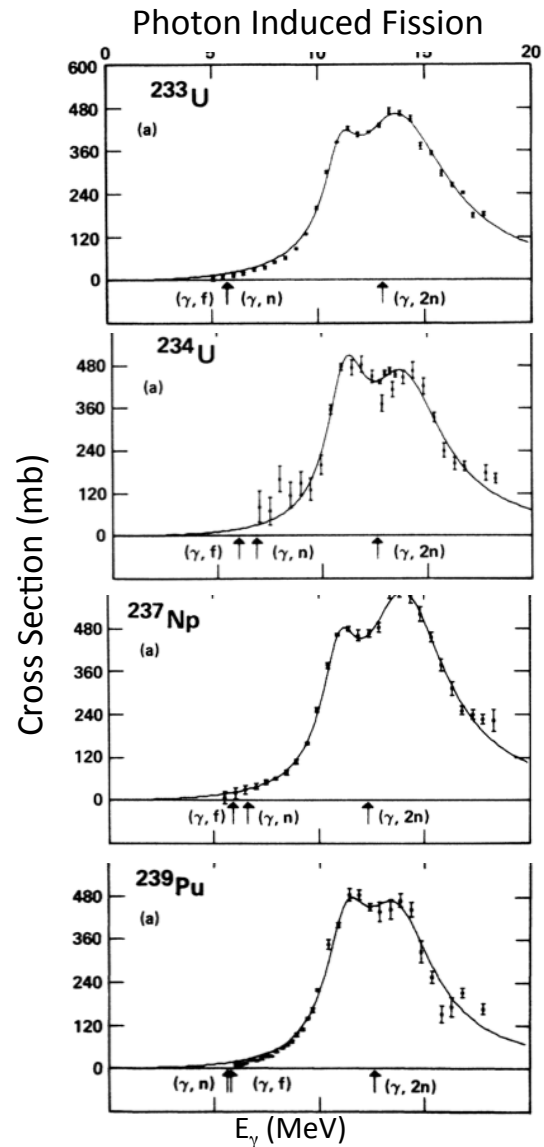


ENDF/B-VII.1

<http://www.nndc.bnl.gov/sigma/>

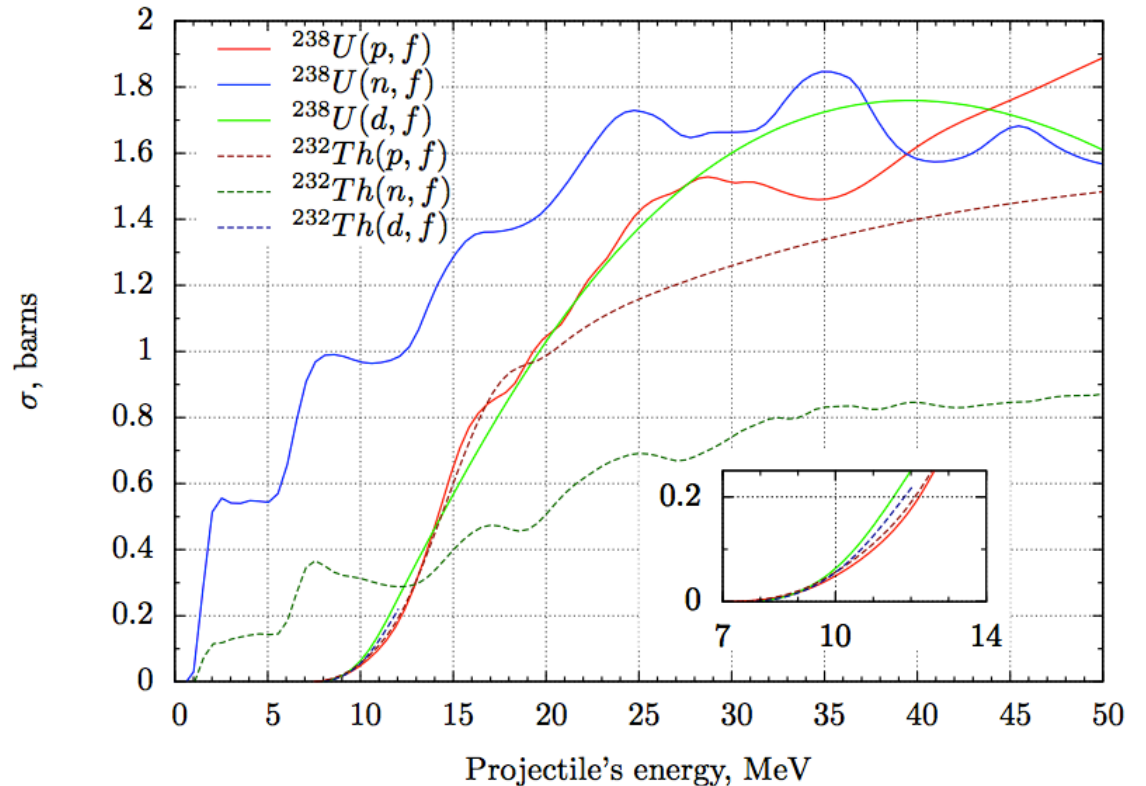
Fission Phenomenology and Observables

Fission induced by other particles than neutrons provide complimentary information



Berman, 1986

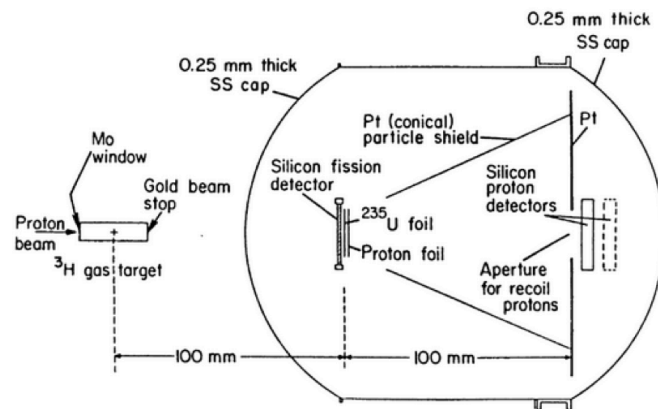
Cross Sections from proton, neutron, and deuteron-induced fission induced fission



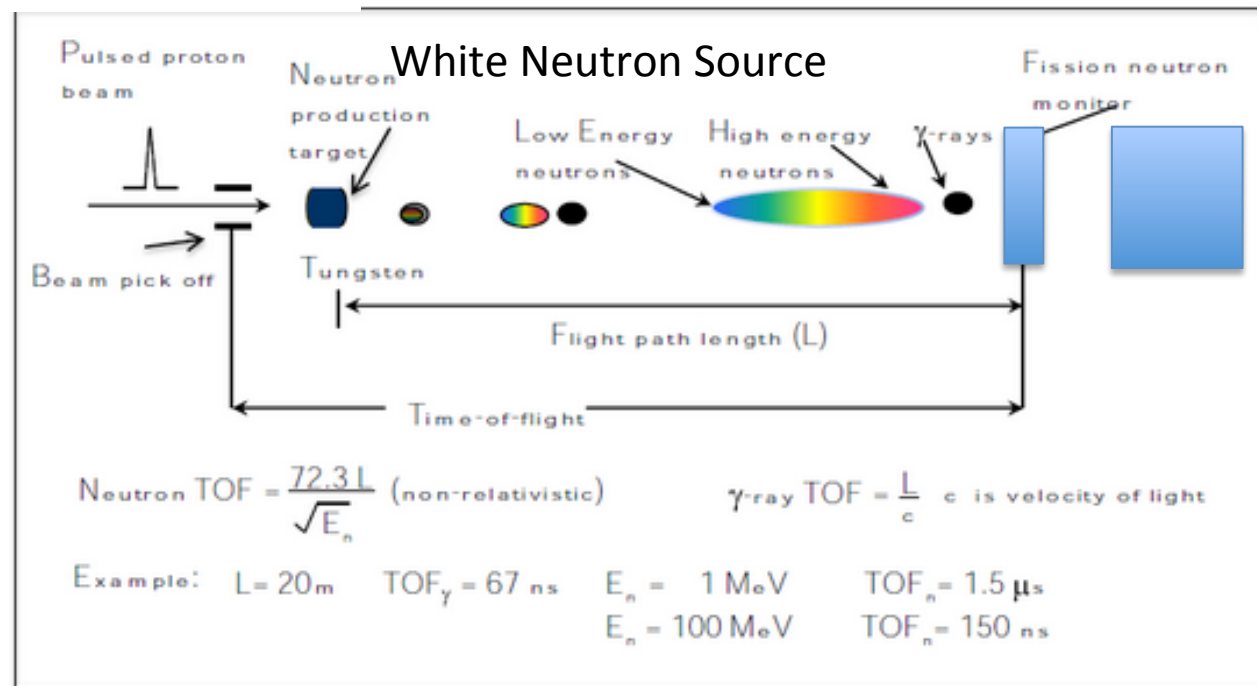
"Nuclear fission studies with the IGISOL method and JYFLTRAP", D. Gorelov Dissertation (2015)

Neutron-Induced Fission Cross Section Measurement Techniques

Typical Fission Neutron Cross Section Arrangements



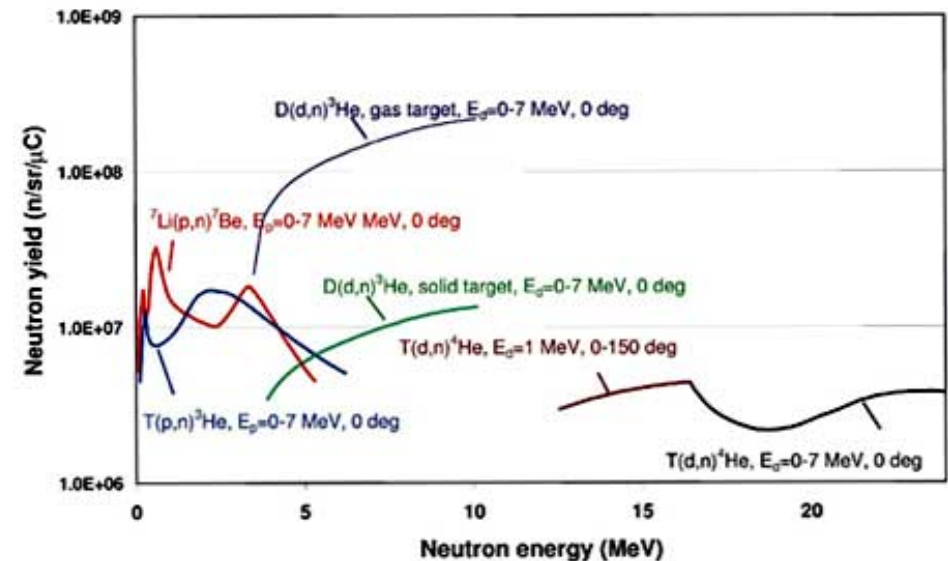
Monoenergetic Neutron Source



Fission Cross Section Measurement Techniques

Neutron Sources – mono-energetic or quasi mono-energetic

Mono-energetic or quasi mono-energetic neutron sources are generally made through light-ion reactions such as $T(d,n)$, $T(p,n)$, $D(d,n)$, ${}^7\text{Li}(p,n)$ and ${}^9\text{Be}(p,n)$ and are generally good sources for fast neutron measurements. Inverse kinematics such as $H({}^7\text{Li},n)$ can be used.



The most common accelerators used for mono-energetic neutron production are Van de Graaff machines, examples used for neutron physics are:

Facility	Particles	Max Energy	Pulse Width	Typ. Beam Current
Triangle Universities Nuclear Laboratory (TUNL) at Duke University	H,D	20 MeV	1 ns	1 – 5 μA
Edwards Accelerator Laboratory at Ohio University	H, D, ${}^3\text{He}$, ${}^4\text{He}$	9 MeV	1 ns	1 – 3 μA
Institute for Reference Materials and Measurements (IRMM), Geel Belgium	H,D	14 MeV	2 ns	1 – 3 μA

Fission Cross Section Measurement Techniques

Neutron Sources – White Neutron Sources and Reactors

Multi-spectral neutron sources generally use energetic beams of protons or electrons striking neutron production targets. Neutron energies are then determined using time-of-flight techniques over relatively long flight paths to allow studies as a function of neutron energy..

Examples of neutron sources available to users for fission research:

Facility	Particles	n Energy	n Pulse Width	Flight Paths
LANSCCE-WNR	800-MeV p	0.1- 600 MeV	0.5 ns	6-25 m
LANSCCE-Lujan	800-MeV p	Thermal – 0.1 MeV	125 ns	6-25 m
GELINA	100 MeV e ⁻	Subthermal – 20 MeV	1 ns	10 – 400 m
RPI	100 MeV e ⁻	0.01 eV to 1 keV	6 ns	25 m
nTOF (CERN)	20 GeV p	meV – GeV	6 ns	185 m

Facilities such as the Lohengrin spectrometer at the ILL reactor allow unique spectroscopic measurements of mass and isotopic yields for fission products.

Fission Cross Section Measurement Techniques

Types of Fission Fragment Detectors

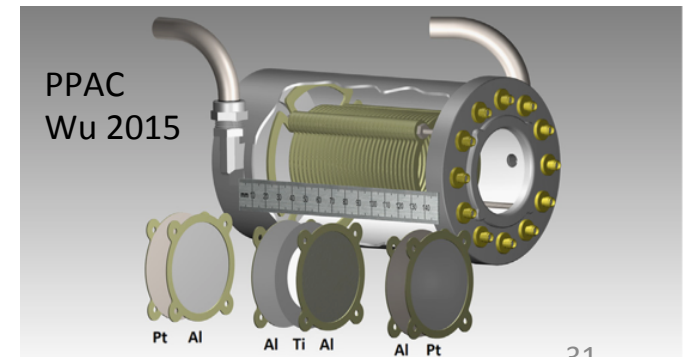
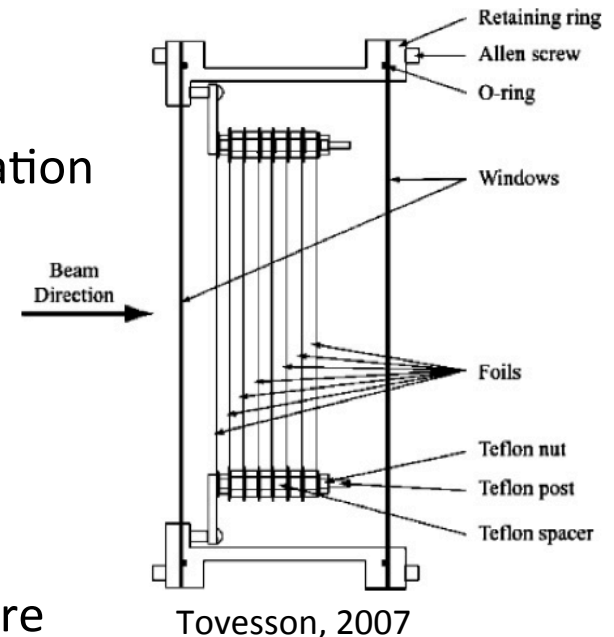
Proportional Counters - most common technique
Parallel plate chamber for fragment detection
Gridded to improve S/N and for angular information

Parallel-plate avalanche counter (PPAC)
Low energy resolution
Very fast response (sub ns)

Gas scintillation chambers
Noble gas mixtures (90% ^3He , 10% Xe) at pressure
Fast response, Large solid angle

Solid-state silicon detectors
Good pulse height information and timing
Good energy resolution, Small solid angle

Time Projection Chamber



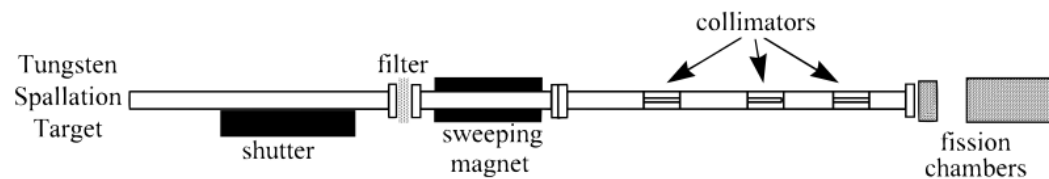
Fission Cross Section Measurement Techniques

Neutron Beam and Flight Path Considerations

- Time marker for pulse generation t_0
- Adequate Collimation -Illumination of fission mass uniformly without having neutrons striking structure
- Removal of potential neutron beam contaminants

Charged particles, gamma rays
Frame overlap for pulsed beam measurements

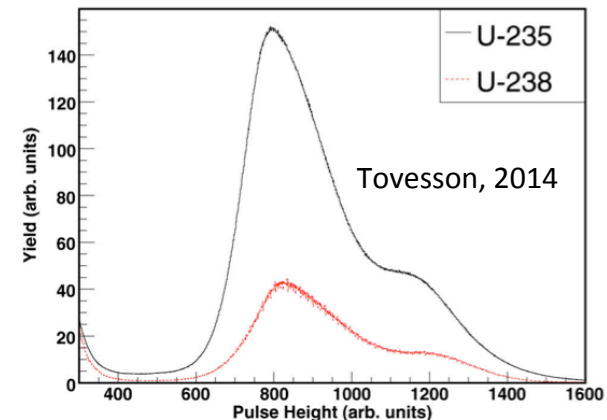
- Incident neutron beam quality
Uniformity, extent at experiment
- Adequate shielding
neutron beam dump
Adjacent flight paths (sky shine)
- Appropriate neutron flight path length



Neutron Flight Path at WNR

Fission Fragment Detection

- Accurate determination of fission foil masses, isotopics, and uniformity
- Adequate electronics for pulse height and timing and gain stability
- Adequate fission-fragment to decay alpha pulse height separation
- Cooling if needed to reduce Doppler broadening in resonance region



Parallel Plate ion Ionization
Chamber Fission Fragment
Response

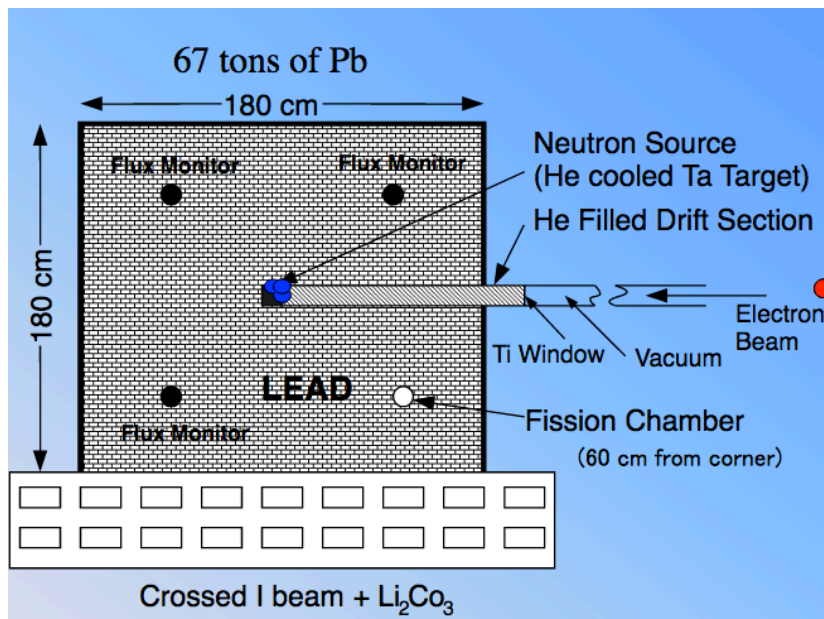
Fission Cross Section Measurement Techniques

Lead Slowing Down Spectrometer (LSDS)

Neutrons are produced by a multi-spectral pulsed neutron source inside a large block of lead. Useful for measuring fission cross sections of quantities of actinides too small for other techniques. This technique is especially useful for small (ng to μg) samples and highly radioactive materials over the energy range 0.1 eV to 100 keV

LSDS sources are possible at RPI, j-PARC, and WNR (Target-2):

LSDS at RPI Linac

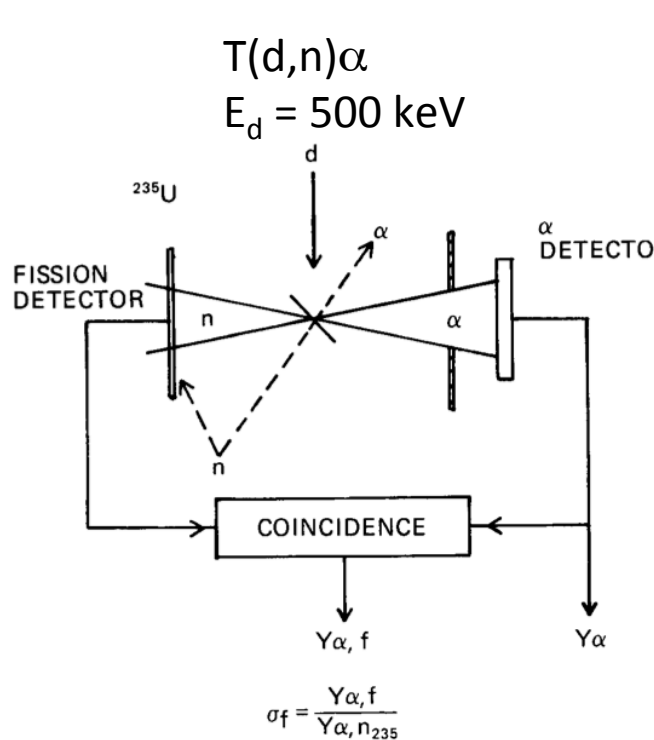


- Ta target at center produces neutrons
- Neutrons slow down by elastic and inelastic scattering
- Neutrons produce a broad high-intensity, 30-40% resolution pulse
- Neutrons traverse the detector multiple times so the flux is 10^3 - 10^4 higher than that on a flight path of equivalent time-of-flight resolution (5.6 m)

Fission Cross Section Measurement Techniques

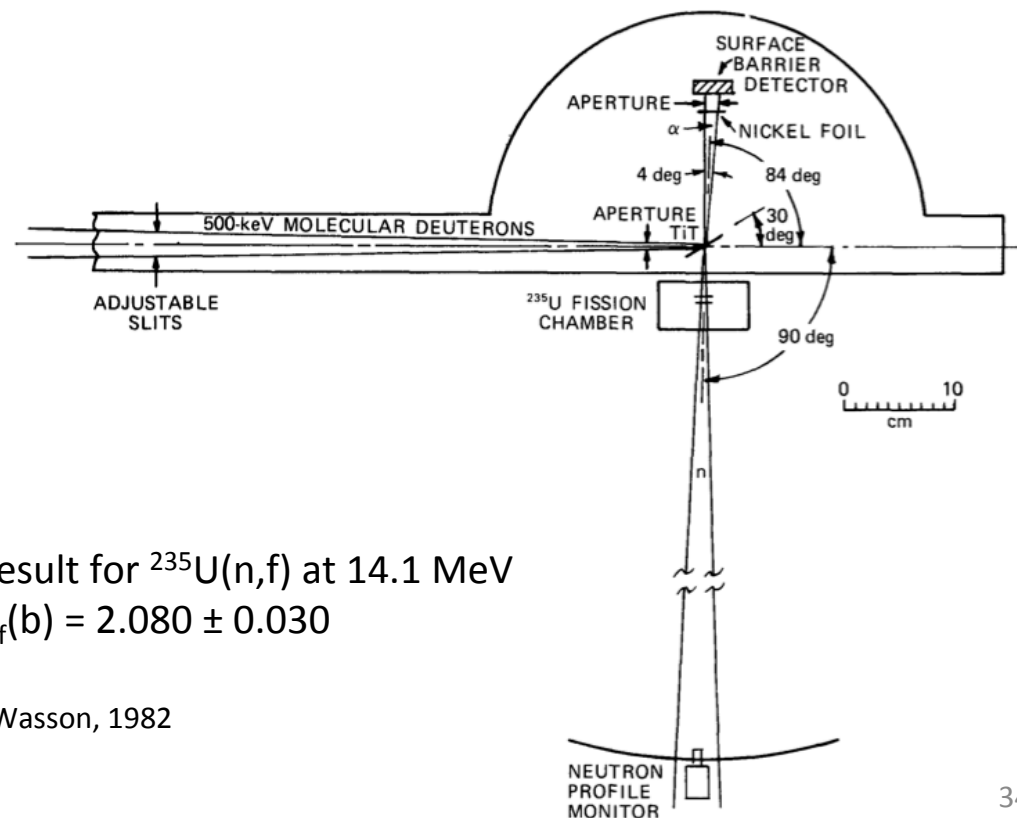
Absolute fission cross section data require an accurate neutron flux measurement

- Use of reference cross section standards $H(n,p)$, ${}^6\text{Li}(n,\alpha)$ (www-nds.iaea.org/standards/)
- Black detector
- Activation Foils
- Associated particle technique (monoenergetic sources)

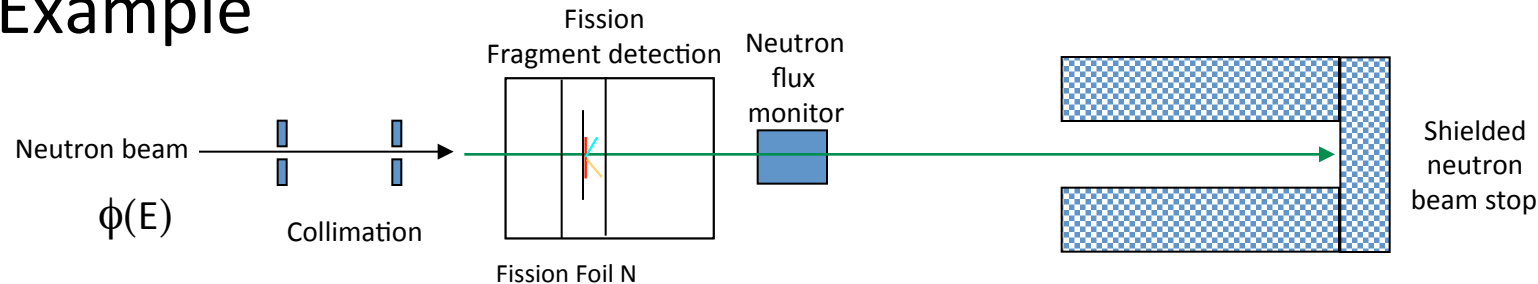


Result for ${}^{235}\text{U}(n,f)$ at 14.1 MeV
 $\sigma_f(b) = 2.080 \pm 0.030$

Wasson, 1982



Fission Cross Section Measurement White-Source Example



In an ideal fission experiment the rate of events is given by: $R(E) = \sigma(E) \cdot N \cdot \phi(E)$

Collecting events for a fixed time: $C(E) = \int \sigma(E) \cdot N \cdot \phi(E) dt = \sigma(E) \cdot N \cdot \Phi(E)$

Where $\Phi(E)$ is the integrated neutron flux and $\sigma(E)$ is the fission cross section .

In a real experiment, the number of events is influenced by the system livetime ($\omega(E)$), the efficiency with which the fission fragments are detected, $\eta(E)$, and any background events $C_b(E)$, so $C(E) = \omega(E) \cdot [N \cdot \sigma(E) \cdot \eta(E) \cdot \Phi(E) + C_b(E)]$

For a pure sample, the cross section is: $\sigma(E) = [1/\omega(E) \cdot C(E) - C_b(E)] / [N \cdot \eta(E) \cdot \Phi(E)]$

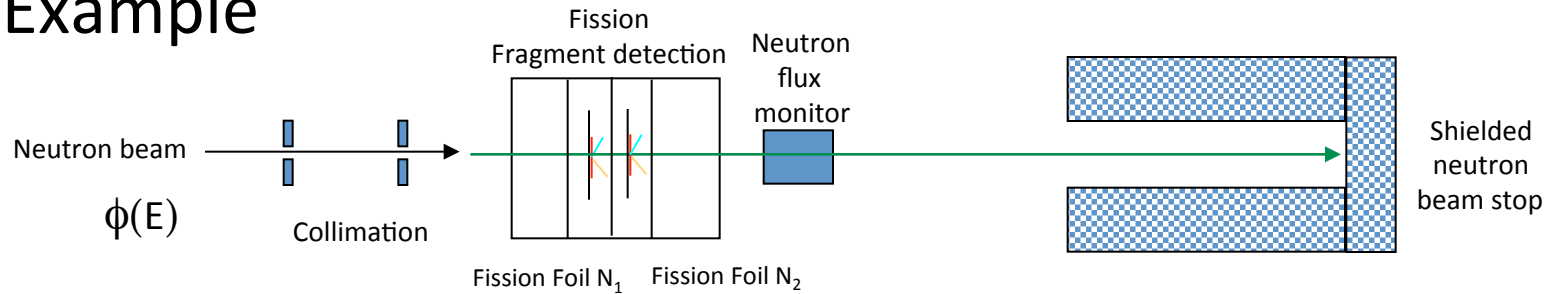
Any fissionable impurities in the sample contributing to the events counted. As a result:

$C(E) = \omega(E) \cdot [\eta(E) \cdot \Phi(E) \cdot N \cdot \{ \sigma(E) + \sum (N_i \cdot \sigma_i(E)) \} + C_b(E)]$ where the $\sum (N_i \cdot \sigma_i(E))$ is the contribution from impurity fission cross sections. Then:

$$\sigma(E) = [1/\omega(E) \cdot C(E) - C_b(E) - \sum (N_i \cdot \sigma_i(E))] / [N \cdot \eta(E) \cdot \Phi(E)]$$

Fission Cross Section Measurement Ratio

Example



In order to avoid the problem of absolute flux determination, fission cross sections are often measured as ratios to a standard fission cross section, such as ^{235}U .

In that case:

$$\sigma_1(E) = [1/\omega_1(E) \cdot C_1(E) - C_{1b}(E) - \sum (N_{1i} \cdot \sigma_{1i}(E))] / [N_1 \cdot \eta_1(E) \cdot \Phi_1(E)]$$

$$\sigma_2(E) = [1/\omega_2(E) \cdot C_2(E) - C_{2b}(E) - \sum (N_{2i} \cdot \sigma_{2i}(E))] / [N_2 \cdot \eta_2(E) \cdot \Phi_2(E)]$$

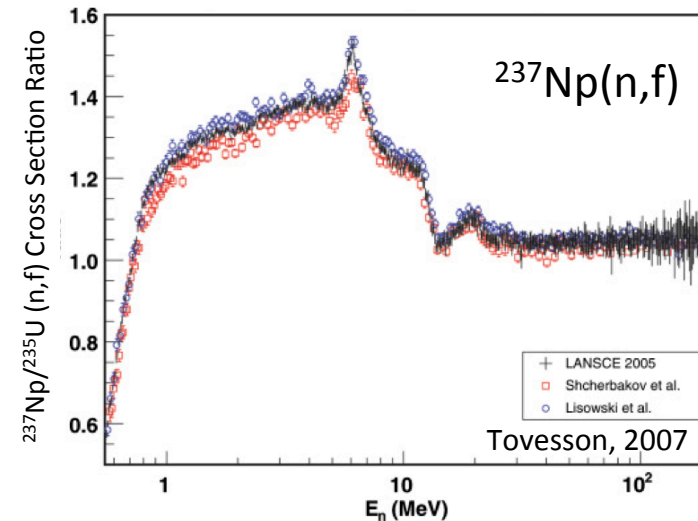
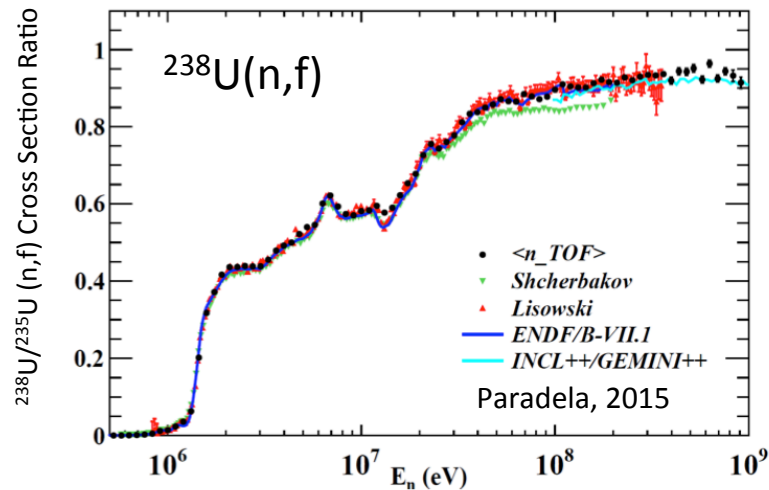
And the cross section ratio is:

$$\frac{\sigma_1(E)}{\sigma_2(E)} = \frac{(N_2 \cdot \eta_2(E) \cdot \Phi_2(E))}{(N_1 \cdot \eta_1(E) \cdot \Phi_1(E))} \cdot \frac{(1/\omega_1(E) \cdot C_1(E) - C_{1b}(E) - \sum (N_{1i} \cdot \sigma_{1i}(E)))}{(1/\omega_2(E) \cdot C_2(E) - C_{2b}(E) - \sum (N_{2i} \cdot \sigma_{2i}(E)))}$$

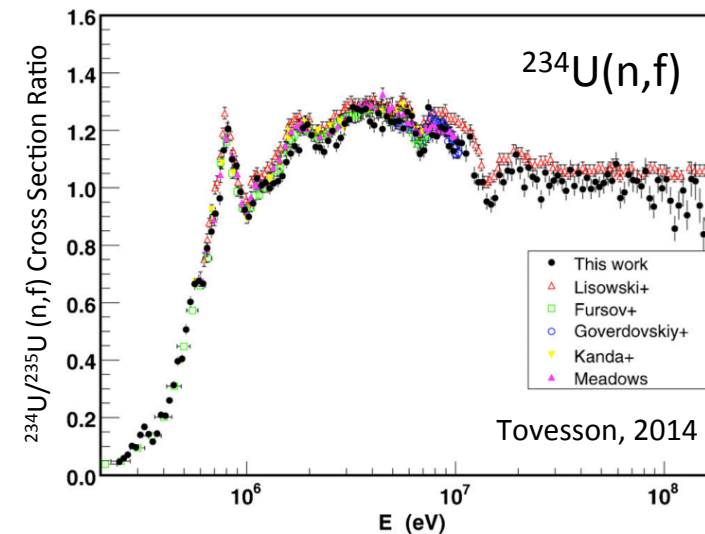
Although this looks like a complication to the absolute cross section measurement, it avoids the necessity of a completely independent determination of the neutron flux, and in a well-designed experiment, many of the quantities in the measurement result in small corrections

Fission Cross Section Ratio Measurements

8

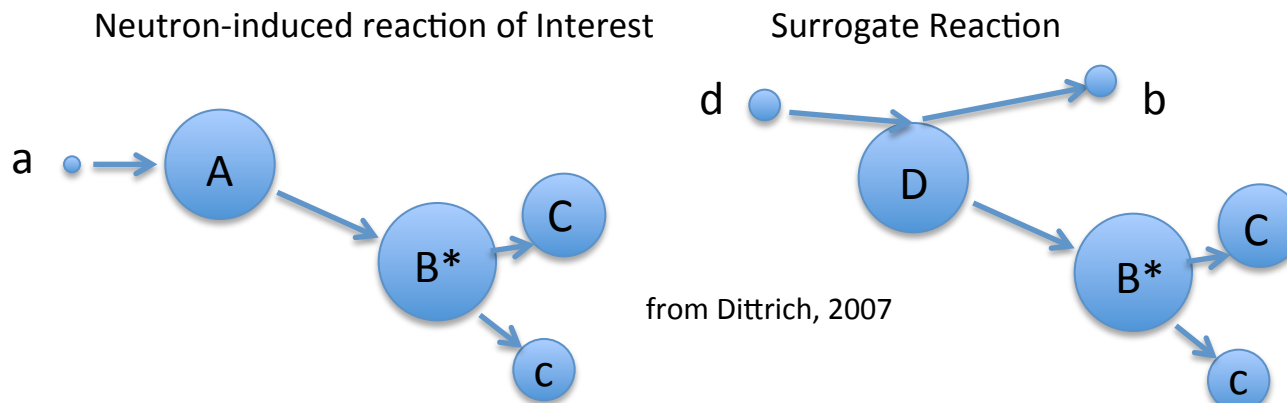


- Ratio measurements offer the best opportunity for low systematic error.
- For $^{238}\text{U}/^{235}\text{U}$ all recent ratio data are in good agreement
- There are still differences of order 3 – 5% for many other ratio data



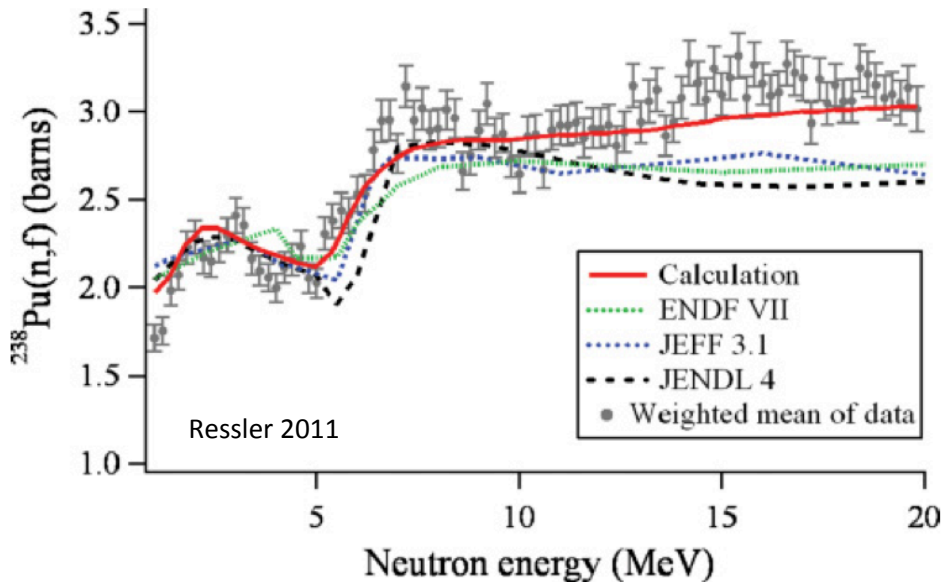
Surrogate Cross Section Techniques Using Charged Particle Reactions

- Many minor isotopes important to fission technology or to theoretical understanding of fission are hard to obtain in sufficient quantity or too short half-lives for a direct neutron measurement.
- A light-ion charged particle reaction is used to form the same compound system B^* as in neutron-induced fission.

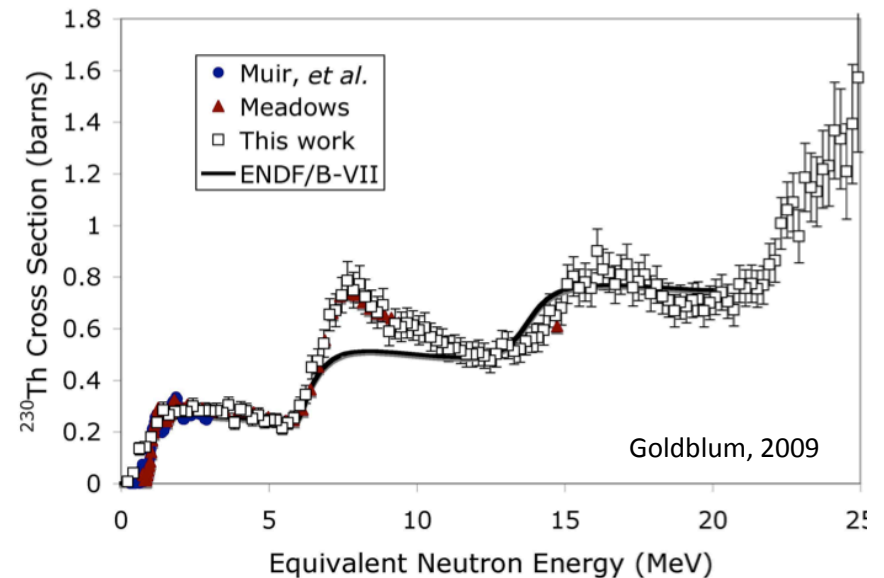


- The decay of B^* is detected in coincidence with the reaction product b . The energy of b fixes E^* , the excitation energy of B^* .
- Hauser Feshbach formalism is then used to correct for the different population mechanisms and produce estimated neutron-induced fission cross sections.

Surrogate Cross Section Techniques Using Charged Particle Reactions - Examples



Surrogate Ratio Method Determination of $^{238}\text{Pu}(n,f)$ cross section from $^{235}\text{U}(\alpha,\alpha'f)$ and $^{236}\text{U}(\alpha,\alpha'f)$ reactions.



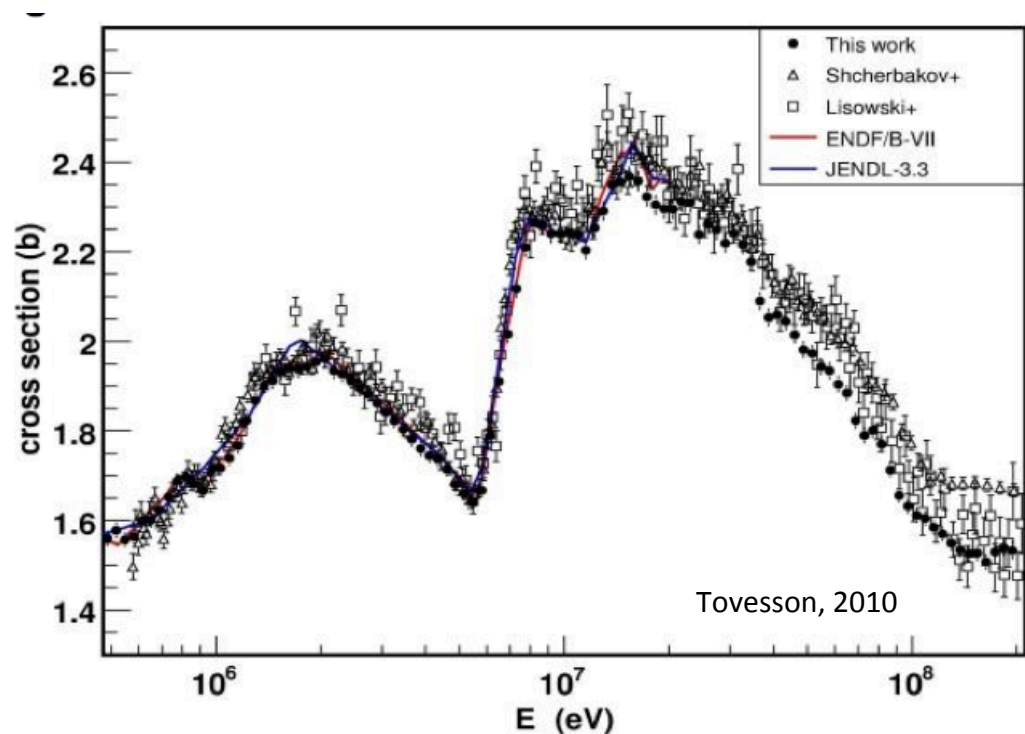
Surrogate Ratio Method Determination of $^{230}\text{Th}(n,f)$ cross section from $^{232}\text{Th}(^3\text{He},\alpha f)$ and $^{234}\text{U}(n,f)$ reactions.

Time Projection Chamber (TPC)

Important fast neutron fission cross sections such as those for $^{239}\text{Pu}(n,f)$ have a 3-6% spread in values for experiments claiming 1-6% uncertainties. This potentially indicates unexplained systematic uncertainties.

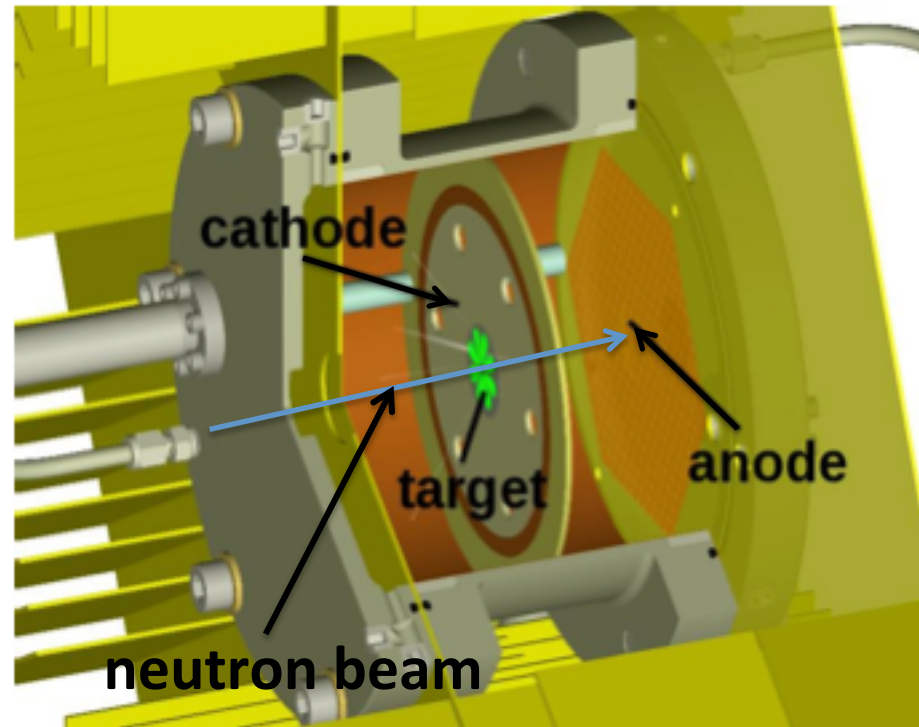
Applications for both national defense and future fast reactor fuel development require more confidence in the actual value.

By incorporating particle tracking techniques developed for high-energy particle detectors, the goal of the TPC collaboration (NIFFTE) is to reduce systematic uncertainties in a credible way to 1% or less for important fission cross sections.



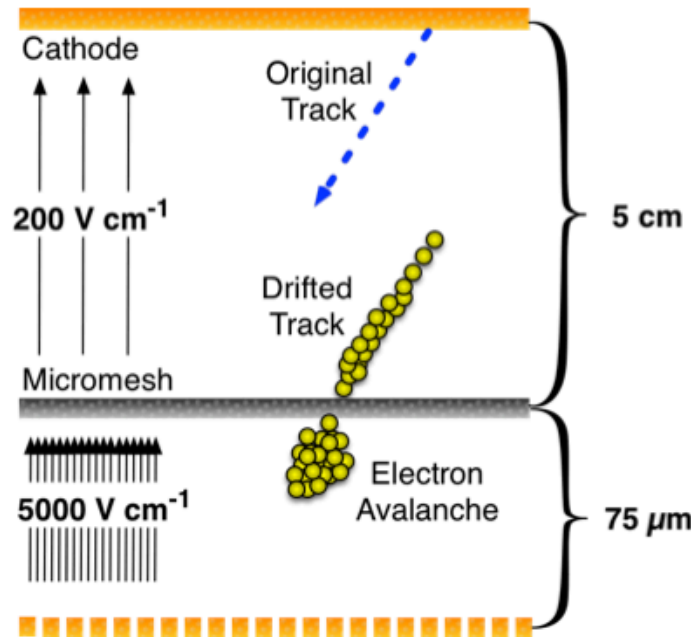
Time Projection Chamber (TPC)

- The TPC uses a two-volume ionization chamber with a segmented anode plane allowing detection of the track of an ionizing particle
- Drift of the ionized gas to a segmented anode gives an x-y signature of the track, and arrival time provides z.
- The ionization profile of the particle track allows particle identification.
- The geometry of the TPC allows nearly 2π coverage of particles emitted from the target.

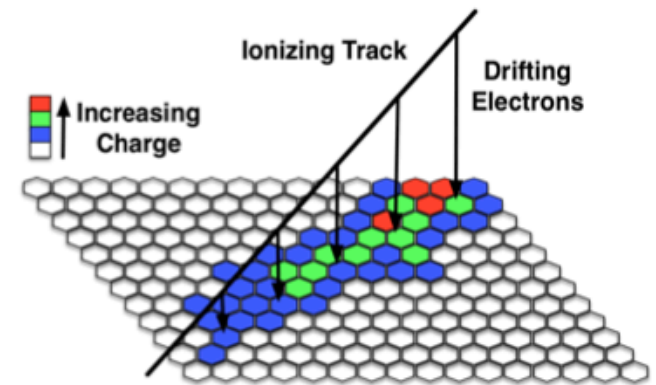


Time Projection Chamber (TPC)

- The TPC uses a two-part system for ionization tracking. Initially the track drifts in a 500 V/cm region
- After drifting 5 cm, the track passes through a micromesh and enters a region with 5000 V/cm, creating an electron avalanche amplification

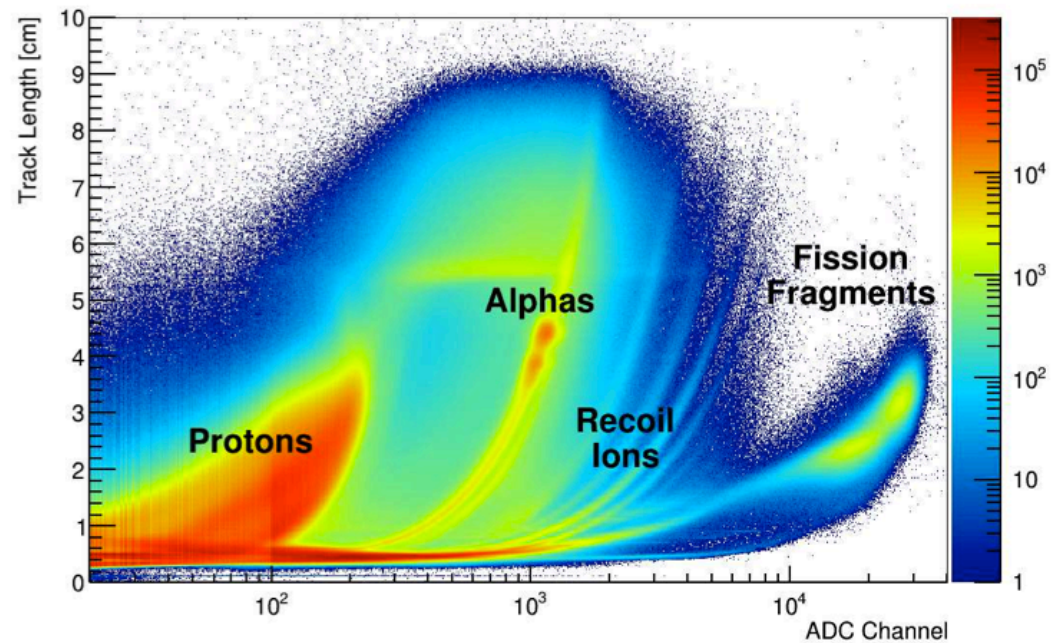
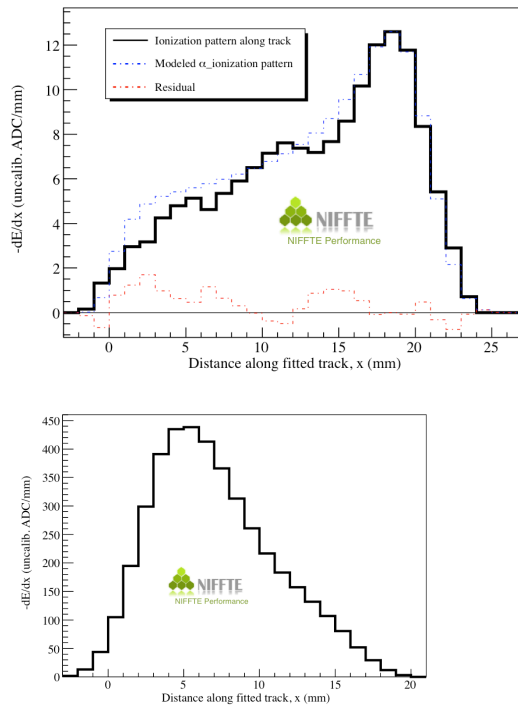


The amplified signal is detected on the anode plane with 5952 hexagonal pads.



A particle ionizes the filling gas and electrons drift towards the segmented pad plane, which provides x and y information while arrival time provides z.

Time Projection Chamber



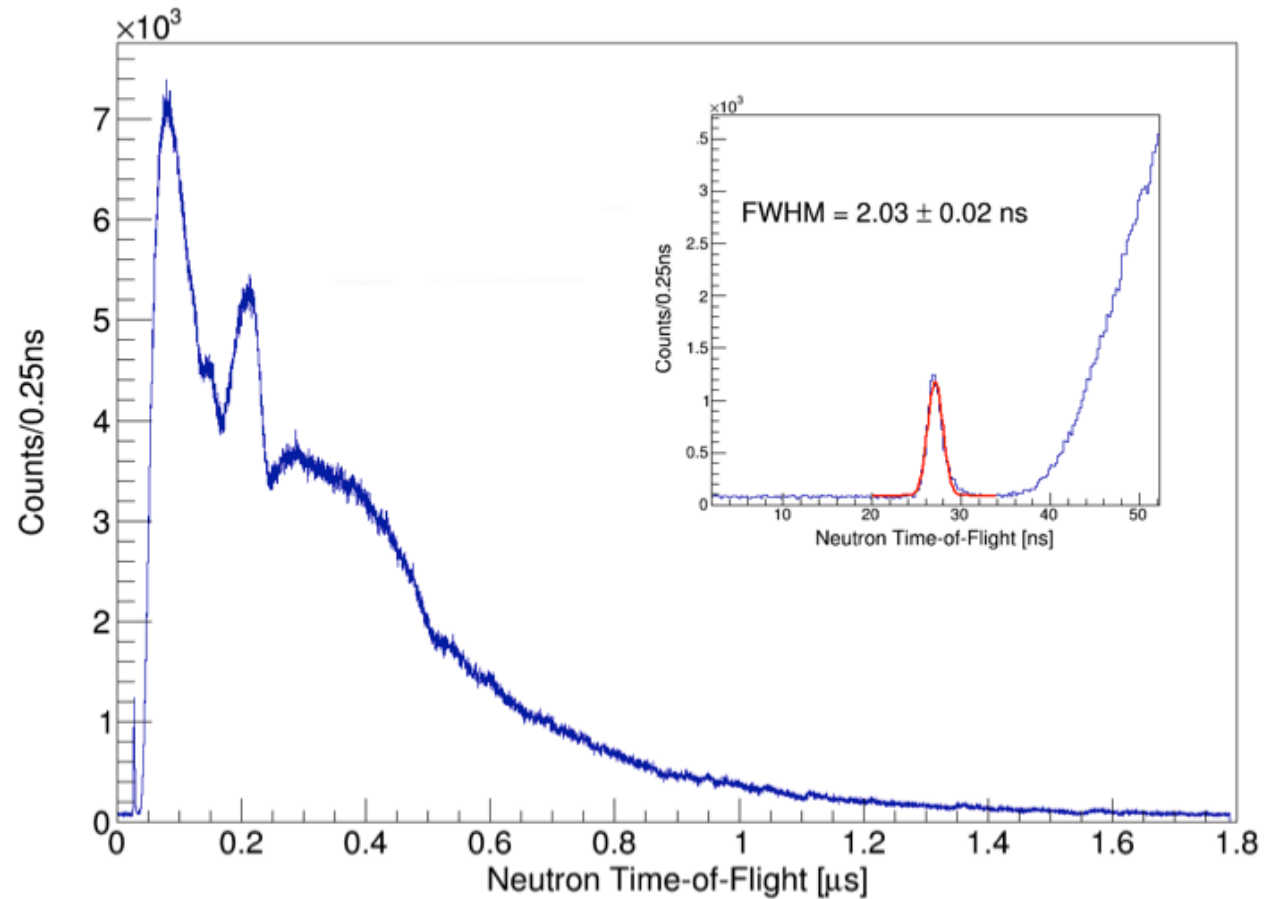
Ionization profiles of decay α and fission products allow particle identification and 2D analysis provides clean separation between the fission fragments from other reactions such as with the argon-isobutane multiplying gas.

Time Projection Chamber (TPC)

- Neutron energy information from time-of-flight
- Energy resolution determined by 2 ns FWHM of target gamma ray pulse

This gives:

E_n (MeV)	ΔE (keV)	%
1	6	0.6
5	70	1.4
10	198	2.0
15	365	2.4
20	565	2.8



Time Projection Chamber (TPC)

- The TPC has the potential to measure high-precision neutron-induced actinide cross sections with an unsurpassed ability to understand all features of the measurement in-situ in order to produce high-accuracy, precision results.
 - Particle identification
 - Target thickness and uniformity
 - Target isotopic content
 - Fragment emission angular distributions
- The TPC has other potential uses:
 - Fission cross sections for binary and ternary fission
 - Fission cross section ratios
 - Neutron-induced reaction cross sections
 - Improved data for cross section standards such as $H(n,p)$, ${}^6Li(n,\alpha)$, ...

The Future of Fission Cross section Measurements and Possible Improvements

- Improved confidence in our current knowledge of neutron-induced fission cross sections, including sufficient information to evaluate covariance data over all energy ranges, is needed for national security applications.
- Development of new fission applications for technology will be a driver for future fission cross section measurements
Generation IV reactors and research on actinide burning systems require better accuracy in both data and higher confidence in evaluations. Some measurements may be possible with a LSDS for very small or highly radioactive samples.
- Continued use of the surrogate technique for actinide fission where samples are unsuitable for direct measurement
- The Time Projection Chamber is a significant step forward in our ability to make accurate and precise measurements because of the increased ability to understand the target and detection process in detail.
Once fully developed, expanding the energy range of the TPC to lower energies would allow measurements in an energy range with significant national security and civilian energy importance.